Carbon residence time dominates uncertainty in terrestrial vegetation responses to future climate and atmospheric CO$_2$

Andrew D. Friend [*], Wolfgang Lucht [†a], Tim T. Rademacher [*], Rozenn M. Keribin [*], Richard Betts [‡], Patricia Cadule [§], Philippe Ciais [¶], Douglas B. Clark [∥], Rutger Dankers [‡], Pete Falloon [‡], Akihiko Ito [**], Ron Kahana [‡], Axel Kleidon [††], Mark R. Lomas [‡‡], Kazuya Nishina [**], Sebastian Ostberg [†], Ryan Pavlick [††], Philippe Peylin [¶], Sibyll Schaphoff [†], Nicolas Vuichard [¶], Lila Warszawski [†] Andy Wiltshire [‡], and F. Ian Woodward [‡‡]

[*]Department of Geography, University of Cambridge, Cambridge CB2 3EN, United Kindgom,[†]Potsdam Institute for Climate Impact Research, Potsdam, Germany, [a]Department of Geography, Humboldt University Berlin, Germany,[‡]Met Office Hadley Centre, Exeter, United Kingdom,[§]Insitute Pierre-Simon Laplace, Paris, France,[¶]Laboratoire des Sciences du Climat et de l'Environnement, Gif-sur-Yvette, France,[∥]Centre for Ecology and Hydrology, Wallingford, UK,[**]National Institute for Environmental Studies, Tsukuba, Japan,[††]Max Planck Institute for Biogeochemistry, Jena, Germany, and [‡‡]University of Sheffield, Sheffield, United Kingdom

Future climate change and increasing atmospheric CO$_2$ are expected to cause major changes in vegetation structure and function over large fractions of the global land surface. Seven global vegetation models are used to analyse possible responses to future climate simulated by a range of GCMs run under all four RCP scenarios of changing concentrations of greenhouse gases. All 110 simulations predict an increase in global vegetation carbon to the end of this century, but with substantial variation between vegetation models. For example, at 4 °C of global land surface warming (510-758 ppmv of CO$_2$), vegetation carbon increases by 52-477 Pg C (224 Pg C mean), mainly due to CO$_2$ fertilization of photosynthesis. Simulations agree on large regional increases across much of the boreal forest, western Amazonia, central Africa, western China, and southeast Asia, with reductions across southwest North America, central South America, southern Mediterranean areas, southwestern Africa, and southwestern Australia. Four vegetation models display discontinuities across 4 °C of warming, indicating global thresholds in the balance of positive and negative influences on productivity and biomass. In contrast to previous global vegetation model studies, we emphasise the importance of uncertainties in projected changes in carbon residence time. We find, when all seven models are considered for one RCPxGCM combination, such uncertainties explain 30% more variation in modeled vegetation carbon change than responses of NPP alone, increasing to 151% for non-HYBRID4 models. A change in research priorities away from production and towards structural dynamics and demographic processes is recommended.

terrestrial ecosystems │ climate change │ CO$_2$ │ residence time │ NPP

Abbreviations: CMIP5, fifth Coupled Model Intercomparison Project; C_{veg}, vegetation carbon; GCM, general circulation model; ΔMLT, change in global mean land surface temperature; GVM, global vegetation model; ISI-MIP, Inter-Sectoral Impact Model Intercomparison Project; NPP, net primary productivity; RCP, Representative Concentration Pathway

Terrestrial vegetation is central to many components of the coupled Earth system, in particular the global carbon cycle, biophysical land-atmosphere exchanges, atmospheric chemistry, and the diversity of life with the numerous ecosystem services this engenders. However, vegetation is very sensitive to climate and levels of atmospheric CO$_2$, the primary substrate for plant growth. Therefore it is imperative that we are capable of anticipating the potential responses of global terrestrial vegetation to future changes in climate and atmospheric chemistry. However, a comprehensive consistent analysis of impacts taking into account uncertainty in both climate models and impacts models has so far been lacking. The recent availability of RCP-driven climate model simulations, with bias-corrected outputs produced within the ISI-MIP project [1], allows such an analysis.

Vegetation biomass, productivity, and the competitive abilities of different plant types are all influenced by climate and atmospheric CO$_2$. Higher temperatures will increase growing season lengths, metabolic rates, and rates of nitrogen mineralisation at high latitudes and altitudes, thereby increasing productivity. However, they may reduce productivity in warmer areas through increased rates of evaporation and stomatal closure due to higher vapour pressure deficits. Increasing atmospheric CO$_2$ will tend to increase rates of photosynthesis and reduce evapotranspiration and/or increase leaf areas. It will also alter tissue stoichiometry, with significant repercussions for herbivores and soil decomposition. Furthermore, higher CO$_2$ will likely increase the competitive ability of plants which use the C3 photosynthetic pathway relative to C4 plants. Plant species have intrinsic ranges of potential water and nutrient use efficiencies, which will affect how they respond, and all plants will acclimate to changed forcings. Biomass is determined by inputs driven by photosynthesis and its allocation and outputs to senescence and mortality, each with their own environmental responses. However, global-scale vegetation model development has strongly focussed on productivity processes whereas, apart from major disturbances such as fire, the dynamics of carbon turnover have been largely ignored.

Beginning in the 1990s, a handful of dynamic global vegetation models (DGVMs) have been developed using parameterisations for many of the processes mentioned above. The first multi-DGVM study to look at the potential impacts of future climate and atmospheric CO$_2$ on global vegetation and soils was reported by [2]. This study looked at the responses of net ecosystem production (NEP), simulated by six DGVMs, to one climate and CO$_2$ change scenario, concluding that the major source of uncertainty in future NEP is the response of NPP to changing climate. Global vegetation carbon was predicted to increase by an average of 240 PgC from pre-industrial levels across the models by 2100, but saturating NPP and increasing heterotrophic respiration led to an eventual reduction in NEP after 2050.

Reserved for Publication Footnotes

Nine global vegetation models (GVMs), four of which were DGVMs, were used in the C^{4}MIP coupled climate-carbon cycle modeling study ([3]). Terrestrial NPP and soil respiration responses to climate and CO_2 dominated the uncertainty of future atmospheric CO_2 levels. [4] looked at the responses of five DGVMs coupled to a fast climate analogue model, finding dramatic divergence in future behavior, particularly of tropical vegetation responses to drought and boreal ecosystem responses to elevated temperature and changing soil moisture. [5] looked in more detail at the responses of three of these DGVMs in the Amazon region, and found that while all simulated reductions in vegetation carbon, they did this for different reasons. LPJ mainly responded to precipitation, HyLand to humidity, and TRIFFID to the direct effects of temperature on physiology.

The main conclusion from these and similar studies is the significant uncertainty due to alternative model formulations of the fundamental physiological processes determining responses of NPP to climate and CO_2. This is perhaps surprising given that physiological processes have been intensively studied for many years, and similar approaches are used in the different models. In fact the basic approaches incorporated into the early DGVMs have hardly changed over time.

Here seven GVMs are used to investigate possible responses of global natural terrestrial vegetation to a major new set of future climate and atmospheric CO_2 projections. This study goes beyond previous work in the range of climate models, scenarios, and GVMs that are considered, and analyses the outputs using an approach that gives equal weighting to production and turnover processes. While all seven models used in the current study have the potential to be DGVMs, only HYBRID4, LPJmL, JeDi, and JULES simulated full vegetation dynamics. ORCHIDEE, SDGVM, and VISIT simulations used prescribed vegetation distributions, and so the model implementations used here are referred to as global vegetation models (GVMs). We discuss the simulated shifts in ecosystem state in terms of underlying model behaviours and assumptions, assess the level of agreement between the GVMs and GVMxGCM combinations, and identify where key uncertainties remain. The overall outcome is a summary of the current state of knowledge concerning the impacts on terrestrial vegetation of future policy decisions that aim to influence anthropogenic greenhouse gas emissions. We recognise that much of the land surface will continue to be transformed by land use, but do not consider this forcing in order to focus on identifying the main discrepancies between vegetation models.

Results

Vegetation Carbon. To facilitate comparison across simulations using all GCMs and RCPs, we express global vegetation change with respect to change in global mean land surface temperature (ΔMLT). It is important to recognise that ΔMLT is a proxy for changing magnitudes of temperature, precipitation, humidity, and CO_2, and that both climate and ecosystem inertia also play roles in the relationships between climate forcing and vegetation responses.

Baseline (i.e. mean 1971-1999) global vegetation carbon (C_{veg}) varies between 461 PgC and 998 Pg C, and increases with ΔMLT for all vegetation models under all 110 climate and CO_2 increase scenarios (Fig. 1) (see Methods for details of simulations). Global C_{veg} increases more-or-less linearly in all models up to about +4 °C, but with different slopes. At higher temperatures four of the models saturate, while the remaining three continue increasing. Inter-model mean C_{veg} stops increasing at +4 °C, where the full range of the increase is 52-477 Pg C, depending on the GVMxGCMxRCP combination. The mean increase of 224 Pg C over all models is equivalant to ≈ 24 yr of recent global fossil fuel CO_2 emissions. Within

GVM variation is largely due to the different GCM climates and CO_2 mixing ratios.

The spatial distribution of the mean response across all 110 realisations that fall into the +4 °C 1-degree wide bin is shown in Fig. 2. Despite the large spread between simulations, consistent spatial patterns are evident. Most land supports increased vegetation carbon, with simulations agreeing on this increase in many locations. Increases are particularly high across much of northern North America, northwestern and southeastern South America, the colder regions of western Europe, most of northern Eurasia, southern Asia, and tropical Africa.

There are also conspicuous regions where vegetation carbon declines, including parts of southern North America, much of central South America, the southern Mediterranean region, southwestern Africa, and southwestern Australia. Declines range to -59% of current C_{veg}. The realisations are less in agreement concerning these declines than they are for regions of increase, except in the northern Maghreb. The spatial extent of the areas experiencing decreased vegetation carbon increases monotonically with warming above +3 °C, as does the inter-model agreement on these reductions. At ΔMLT = +7 °C, very large areas of South America, the Mediterranean region, and Australia experience mean decreases in C_{veg} relative to current values. Moreover, model agreement at the 90% level extends to southwestern Africa and Australia at these higher temperature increases. In contrast, model agreement on increases at +7 °C becomes more confined than at lower warming, with the Tibetan Plateau, Ethiopean Highlands, northeastern Siberia, and southwestern Canada still consistently experiencing higher C_{veg}. In addition, we find that an extensive region of the southern Sahara/northern Sahel experiences very large relative increases in vegetation carbon, although there is less agreement on this between simulations, primarily due to variation in climate predictions.

Inter-simulation variation is greatest for C_{veg} change between current and +4 °C-binned simulations across central USA, northeastern South America, southern Africa, the near East, and much of Australia. These tend to be regions with increasing future moisture stress, which is inconsistently simulated by the GCMs.

Model Differences. Focussing on the results from one of the GCMxRCP scenarios allows vegetation model behaviour to be analysed in more detail. The mean global land surface temperature in the HadGEM2-ES RCP 8.5 simulation rises to ≈ 7.5 °C above current values, covering almost the entire spread of all GCMxRCP forcings. Furthermore, the global C_{veg} responses under this forcing (Fig. 3) are close to the mean responses of each vegetation model across all forcing scenarios. Global C_{veg} increases remarkably linearly throughout the century in five vegetation models (i.e. ORCHIDEE, JeDi, JULES, SDGVM, and VISIT). In contrast, in LPJmL and HYBRID4 global C_{veg} saturates by about 2050, followed by a decline. Similar behaviors, against temperature, are evident in Fig. 1.

Changing C_{veg} results from changes in NPP and the residence time of carbon in living vegetation

$$\frac{dC_{veg}}{dt} = NPP - \frac{C_{veg}}{\tau} \qquad \textbf{[1]}$$

where τ is the carbon residence time. This formulation is applied here both locally and globally as a difference equation over annual timesteps, enabling annual residence time to be inferred from simulated NPP and ΔC_{veg}. In the vegetation models used here, NPP is responsive to climate and atmospheric CO_2, both directly and through indirect effects on vegetation development. Carbon residence time depends on the turnover rates of plant parts and the mortality rates of individuals, processes modeled with both fixed background components, climate sensitivities, including fire, competitively-induced mortality, and are affected indirectly through shifts in vegetation composition, although not all these processes are treated in all models.

All models except HYBRID4 display a highly linear increase in global NPP with time (Fig. 3). This linear increase is due to a saturating effect of CO_2 combined with a near-linear negative impact of climate change. In contrast, global mean annual residence time either declines (JeDi, VISIT, JULES, and LPJmL), increases (HYBRID4 and ORCHIDEE), or does not change (SDGVM). Residence time in LPJmL remains fairly constant until about 2050, and then declines rapidly, whereas in VISIT it stabilises in 2050 and in HYBRID4 it then increases more rapidly. These results suggest that the primary causes of the differences in the trajectories of future global C_{veg} between the GVMs are the different ways in which residence time responds to climate and CO_2, at least for the non-HYBRID4 models. This suggests that analyses of differences in model behaviour should focus not only on the processes of carbon acquisition (i.e. photosynthesis and NPP), but at least as much on the dynamics of vegetation carbon turnover.

Using additional simulations with each GVM in which the CO_2 experienced by the vegetation was held constant, these results were further analysed by fitting to each GVM globally, a simple two-parameter model for the relationship between NPP and CO_2 (i.e. $a_1 \Delta C_a / (a_2 + \Delta C_a)$, where ΔC_a is the change in CO_2), combined with linear models for the relationships between NPP and temperature (i.e $a_3 \Delta MLT$), and residence time and temperature (i.e. $a_4 \Delta MLT$). The fitted global model is plotted as lines on Fig. 3, and is used to ascribe sources of uncertainty to different processes. The variance in final C_{veg} caused by differences in fitted residence time relationships between models was found to be 30% higher than that caused by differences in the fitted NPP responses when all models were considered. Leaving out HYBRID4, which displays a different NPP response, increases the effect of residence time to 151% more than that of NPP. In other words, for the non-HYBRID4 models, differences in residence time relationships with climate between the models are responsible for more than twice the variation in modeled global C_{veg} change to 2100 than are differences in NPP relationships with temperature and CO_2.

The HYBRID4 vegetation model includes a nitrogen cycle, and so this might be expected to be the reason for the decline in NPP, and hence C_{veg}, above 4 °C of warming because of the potential for nitrogen to limit CO_2 fertilization (e.g. [6]). However, further analysis showed that the decline in NPP is in fact due to increased vapour pressure deficits causing stomatal closure and increased evaporative demand over temperate and tropical forests, with increasing nitrogen mineralization reducing the potential constraint from N feedbacks (Fig. 4). There is considerable variability in the ways in which stomata respond to humidity between the models.

In contrast, the decline in C_{veg} after 2050 in LPJmL is driven by increases in turnover across the temperate and boreal forests (Fig. 4). Tree mortality increases as a consequence of increasing tissue mortality due to high temperature periods, and in response to water stress in these regions, with subsequent increasing transient dominance by C3 grasses during slow re-growth of better-adapted tree types.

Declining residence times in JeDi, LPJmL, JULES, and VISIT with warming, as shown in Fig. 4, would by themselves lead to reduced C_{veg}, but these changes are more than compensated for by increases in NPP at the global scale (Fig. 3). Declining residence times in these models are due to temperature-dependencies of turnover rates (processes included in the models and important for production and residence time differences are indicated symbolically on Fig. 4). In contrast, global mean residence time in HYBRID4 and ORCHIDEE increases. In HYBRID4 this is due to reduced tree mortality across the boreal forest as higher CO_2 concentrations and temperatures improve their carbon balance. Residence time of temperate and Amazon forest carbon in HYBRID4 is reduced with warming due to heat-induced increases in vapour pressure deficits leading to unfavourable carbon balances, which increase rates of individual mortality (Fig. 4). In ORCHIDEE residence time increases across

much of the boreal forest and many tropical regions. These changes are due to a greater biomass of younger leaves, which increases with NPP, and has lower intrinsic rates of turnover than older leaves.

In JeDi, residence time falls over much of the northern boreal and arctic region, as well as the tropics, whereas it increases across temperate latitudes (Fig. 4). In contrast, in JULES residence time decreases in across mid-latitudes deciduous forests, but changes little elsewhere. These changes are driven by changing vegetation types mixtures, with grasses and smaller shrubs in JeDi decreasing boreal residence times, and greater proportions of trees increasing residence times in southeastern USA and China. In VISIT, reductions in tropical residence time occur in response to increased fire frequency.

Discussion

Using simulation results from five GCMs and the full range of RCPs, we have characterised the range of terrestrial vegetation responses to future conditions across seven different global vegetation model formulations. However, multiple sources of uncertainty in the chain from climate forcing to impact model limit confidence in specific predictions. Agreement nevertheless emerges on increases in future global vegetation carbon, with large regional increases across much of the boreal forest, western Amazonia, central Africa, western China, and southeast Asia. Simulations also agree on decreases in parts of northern Africa. Furthermore, there is agreement on a general increase in the areal extent of regions with negative impacts above +3 °C of warming. The relative dominance of different plant types is also predicted to change, but there is little consensus among the models as to the details.

Previous modeling studies have also consistently predicted increased global vegetation carbon under future scenarios of climate and CO_2, but with considerable variation in absolute values ([2], [3], [4]). A relatively large additional land carbon pool has been viewed as implausible due to N constraints on additional plant growth ([7], [6]). However, N constraints in this study are not responsible for different responses to forcings. Nevertheless, better understanding of nutrient constraints in general, and how to incorporate them into global vegetation models, is a major priority. Observational evidence strongly suggests that global vegetation carbon in natural forests is already increasing ([8]), and the relationship of any future increases with ΔMLT has important consequences for future levels of atmospheric CO_2. The results presented here provide new constraints on the likely range under different amounts of global mean warming.

Analysing the global and local responses of the GVMs in terms of the responses of carbon inputs (i.e. NPP) and outputs (i.e. 1/residence time) to climate and CO_2 helps to identify sources of model differences. Changes in NPP are more consistent between models than changes in residence time, which either increases, decreases, or does not change over this century. Two of the GVMs, LPJmL and HYBRID4, treat competitive interactions explicitly, either through competition between plant types (LPJmL), or between actual individuals using a gap model approach (HYBRID4), with increased mortality resulting from competition. However, residence time in these two models changes in opposite directions with respect to climate change. In contrast, it was found that when CO_2 was fixed residence time declined with warming in both HYBRID4 and LPJmL, albeit with a significantly greater reduction in the latter model. The switch in the sign of response in HYBRID4 is due to the removal of the beneficial effects of increasing CO_2 on tree survival, leading to increased tree mortality with atmospheric evaporative demand. In JULES, on the other hand, residence time declines with warming when CO_2 also increases, yet increased with warming when CO_2 is fixed. This increase was responsible for JULES having almost no overall change in global C_{veg} when CO_2 was fixed, despite falling NPP. In ORCHIDEE, residence time also increased with warming when CO_2 was fixed, with little overall change in C_{veg}. It is clear from these results that the response of residence time to climate and CO_2 is a

critical yet inconsistently represented feature of current global vegetation models.

While it has been recognised for some time that differences in modeled NPP responses to climate and CO_2 are major sources of uncertainty in GVMs, there has been little discussion on the importance of residence time. A significant component of this key ecosystem characteristic is dependent on relatively slow processes such as rates of recuitment, mortality, and changes in vegetation composition. In contrast, validation exercises have focussed on short-term carbon fluxes and leaf area dynamics, features readily observable (e.g. [9]). However, there is increasing recognition of the importance of demographic processes not just for compositional dynamics, but also for changes in carbon balance (e.g. [10]).

Discontinuities in vegetation responses at around 4 °C of global land surface warming across a number of the vegetation models indicate thresholds above which the positive impacts of increasing CO_2 become dominated by negative impacts of moisture stress at the global scale. In two models the threshold is expressed in NPP, in two it is in residence time, and in one it is in both. Further work should focus on confronting the processes and emergent model behaviour responsible for these discontinuities with observational data. Spatial and temporal variability in carbon residence time and tree mortality is an obvious place to start, and while recent studies have identified important sources of relevant data (e.g. [11], [12], [13]), data on key processes such as mortality at large scales are rare. Vegetation carbon residence time is not only important because of its contribution to GVM uncertainty, it also represents a key stage in the cascade of carbon from the atmosphere, through various organic and inorganic surface pools, and back to the atmosphere. Changes in vegetation carbon residence times can cause major shifts in the distribution of carbon between pools, overall fluxes, and the time constants of terrestrial carbon transitions, with consequences for the land carbon balance and the associated state of ecosystems. The model results presented here demonstrate a need for increased understanding of the multi-facetted dynamics of vegetation carbon residence time.

Materials and Methods

Daily climate forcings for the land area were provided for all four RCPs sub-mitted as part of the fifth phase of the CMIP5 ([14]) from the following five GCMs: GFDL-ESM2M, HadGEM2-ES, IPSL-CM5A-LR, MIROC-ESM-CHEM, and NorESM1-M. The raw daily climate model simulation results were bias corrected according to the ISI-MIP protocol ([15], [1]), despite known caveats with respect to the use of bias correction in climate impact studies ([16]). The above results are based on simulations using these daily climate forcings from the following seven GVMs: HYBRID4 ([17]), JeDi ([18]), JULES ([19]), LPJmL ([20]), ORCHIDEE ([21]), SDGVM ([22]), and VISIT ([23], [24]). In total, 110 simulations have been included in this analysis. The vegetation models were used to simulate the responses of natural terrestrial vegetation to climate and CO_2 mixing ratio changes at $0.5° \times 0.5°$ (except for JULES and JeDi, which were run at $1.25° \times 1.85°$) spatial resolution over 1951-2099.

The total time duration of the spin-up varied among the vegetation models in order to accommodate differences in reaching equilibrium for multiple state variables. As spin-up climatology, the detrended and bias-corrected daily climate inputs for three consecutive decades spanning 1951-1980 were provided for each GCM (JULES used HadGEM2-ES climate for all spin-ups). Except for JULES, if the spin-up required more than 30 years every second thirty year period was inverted (i.e. 1980-1951), to avoid artefacts due to discontinuities in the climate data. The CO_2 mixing ratio during the spin-up and historical periods was fixed at 280 ppmv for all years before 1765, and was thereafter increased linearly until 2005 (2004 for HadGEM2-ES and 2000 for fixed CO_2 runs). CO_2 mixing ratio was then changed according to the RCP until 2099 (or fixed at the 2001 value for the no CO_2 change runs).

1. **ISI-MIP. (2013) The Intersectoral Impact Model Intercomparison Project (ISI-MIP).** *Proceedings of the National Academy of Sciences* xx:xxxx-xxxx.

2. **Cramer W et al. (2001) Global response of terrestrial ecosystem structure and function to CO_2 and climate change: results from six dynamic global vegetation models.** *Global Change Biology* 7:357-373.

3. **Friendlingstein et al. (2006) Climate-carbon cycle feedback analysis: Results from the C^4MIP model intercomparison.** *Journal of Climate* 7:357-373.

4. **Sitch S et al. (2008) Evaluation of the terrestrial carbon cycle, future plant geography and climate-carbon cycle feedbacks using five Dynamic Global Vegetation Models (DGVMs).** *Global Change Biology* 14:2015-2039.

5. **Galbraith D et al. (2010) Multiple mechanisms of Amazonian forest biomass losses in three dynamic global vegetation models under climate change.** *New Phytologist* 187:647-665.

6. **Luo Y et al. (2004) Progressive nitrogen limitation of ecosystem responses to rising atmospheric carbon dioxide.** *BioScience* 8:731-739.

7. **Hungate B, Dukes JS, Rebecca Shaw M, Luo Y, Field CB. (2003) Nitrogen and climate change.** *Science* 302:1512-1513.

8. **Pan Y et al. (2011) A large and persistent carbon sink in the world's forests.** *Science* 333, 988-993.

9. **Randerson JT et al. (2009) Systematic assessment of terrestrial biogeochemistry in coupled climate-carbon models.** *Global Change Biology* 15:2462-2484.

10. **Purves D, Pacala S. (2009) Predictive models of forest dynamics.** *Science* 320:1452-1453.

11. **Allen CD et al. (2010) A global overview of drought and heat-induced tree mortality reveals emerging climate change risks for forest.** *Forest Ecology and Mangement* 259, 660-684.

12. **Lines ER, Coomes DA, Purves DW. (2010) Influences of forest structure, climate and species composition on tree mortality across the Eastern US.** *PloS ONE* 5(10): e13212. doi:10.1371/journal.pone.0013212.

13. **Galbraith D et al. (2013) Residence times of woody biomass in tropical forests.** *Plant Ecology and Diversity* 6:139-157.

14. **Taylor KE, Stouffer RJ, Meehl GA. (2012) An overview of CMIP5 and the experiment design.** *Bulletin of the American Meteorological Society* 93:485-498.

15. **Hempel S, Frieler K, Warszawski L, Schewe J, Piontek F. (2013) A trend-preserving bias correction - the ISI-MIP approach.** *Earth System Dynamics* 4:219-236.

16. **Ehret U, Zehe E, Wulfmeyer V, Warrach-Sagi K, Liebert J. (2012) Should we apply bias correction to global and regional climate model data?.** *Hydrology and Earth System Sciences* 16:3391-3404.

17. **Friend AD, White A (2000) Evaluation and analysis of a dynamic terrestrial ecosystem model under preindustrial conditions at the global scale.** *Global Biogeochemical Cycles* 14:1173-1190.

18. **Pavlick R, Drewry DT, Bohn K, Reu B, Kleidon A. (2012) The Jena Diversity-Dynamic Global Vegetation Model (JeDi-DGVM): a diverse approach to representing terrestrial biogeography and biogeochemistry based on plant functional trade-offs.** *Biogeosciences* 10:4137-4177.

19. **Clark DB et al. (2011) The Joint UK land environment simulator (JULES), model description-Part 2: carbon fluxes and vegetation dynamics.** *Geoscientific Model Development* 4:701-722.

20. **Sitch S et al. (2003) Evaluation of ecosystem dynamics, plant geography and terrestrial carbon cycling in the LPJ dynamic global vegetation model.** *Global Change Biology* 9:161-185.

21. **Krinner G et al. (2005) A dynamic global vegetation model for studies of the coupled atmosphere-biosphere system.** *Global Biogeochemical Cycles* 19, GB1015.

22. **Woodward FI, Lomas MR. (2004) Vegetation dynamics - simulating responses to climatic change.** *Biological Reviews* 79:643-670.

23. **Ito A, Oikawa T. (2002) A simulation model of the carbon cycle in land ecosystems (Sim-CYCLE): a description based on dry-matter production theory and plot-scale validation.** *Ecological Modelling* 151:143-176.

24. **Inatomi M, Ito A, Ishijima K, Murayama S. (2010) Greenhouse gas budget of a cool-temperate deciduous broad-leaved forest in Japan estimated using a process-based model.** *Ecosystems* 13:472-483.
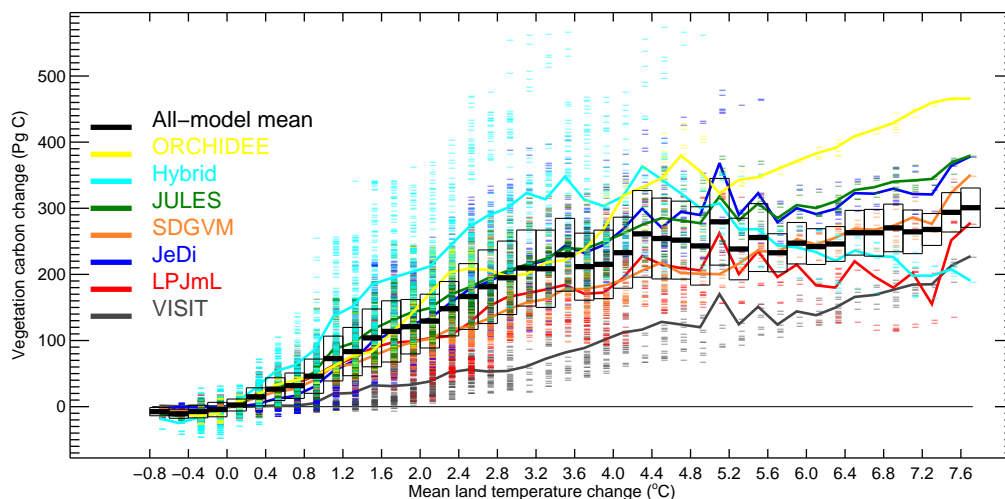
Fig. 1: Future global vegetation carbon change calculated by seven global vegetation models using climate outputs and associated increasing CO_2 from five GCMs run with four RCPs, expressed as the change from the 1971-1999 mean relative to change in global mean land temperature. The annual values for each model are shown for all simulations binned into 0.2-degree wide bins (short, horizontal stripes; n for each bin varies from 6 to 857). The means for each model (thick coloured lines) and the multi-model means and standard deviations (black bars and boxes) are also shown. Average CO_2 in the bins increases from 370 ppmv at ΔMLT = 0 $^{\circ}$C to 911 ppmv at ΔMLT = 7.5 $^{\circ}$C.

Vegetation carbon change between A.D. 1971–1999 and decades with +4 $^{\circ}$C mean land warming (kg C m^{-2})
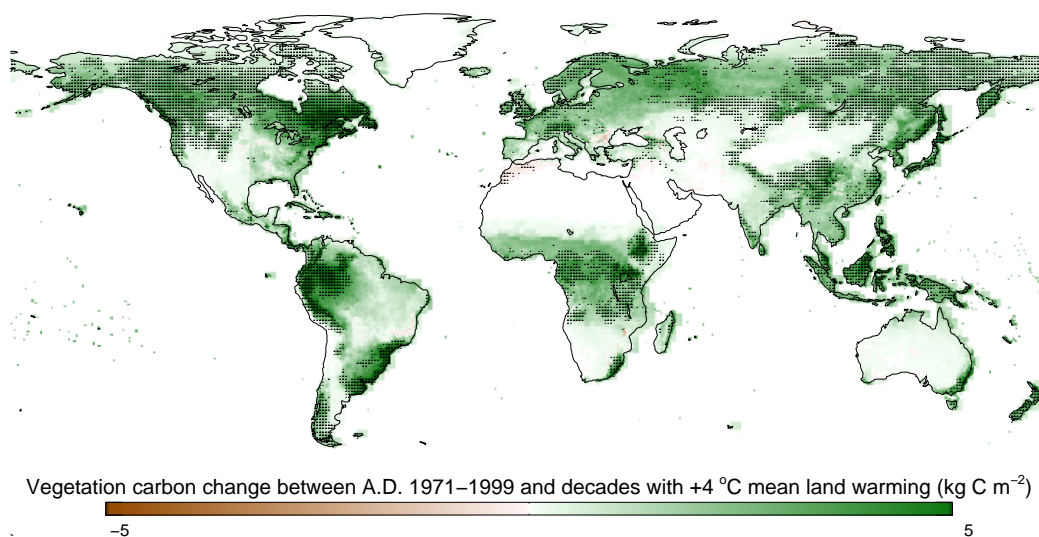
Fig. 2: Mean change in vegetation carbon at +4 $^{\circ}$C global land warming from a 1971-1999 baseline. Values are changes averaged across all simulations and decades (i.e. GVMxGCMxRCPxdecade, n = 110), binned into the mean-decadal 3.5 $^{\circ}$C-4.5 $^{\circ}$C change bin (CO_2 = 510-758 ppmv). Stippling shows where at least 90% of all realisations agree on the sign of change.
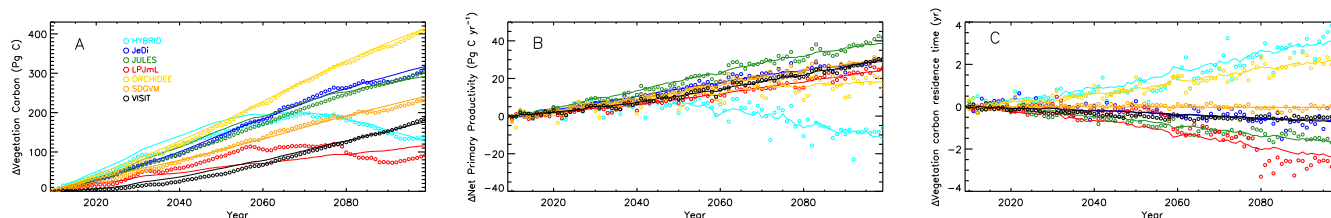
Fig. 3: Change in annual global mean vegetation carbon (A), NPP (B), and residence time of carbon in vegetation (C) under the HadGEM2-ES RCP 8.5 climate and CO_2 scenario for seven global vegetation models. Symbols are GVM outputs and lines are fitted responses using a simple model fitted to the global NPP responses to CO_2 and temperature and residence time responses to temperature for each model as described in the main text.
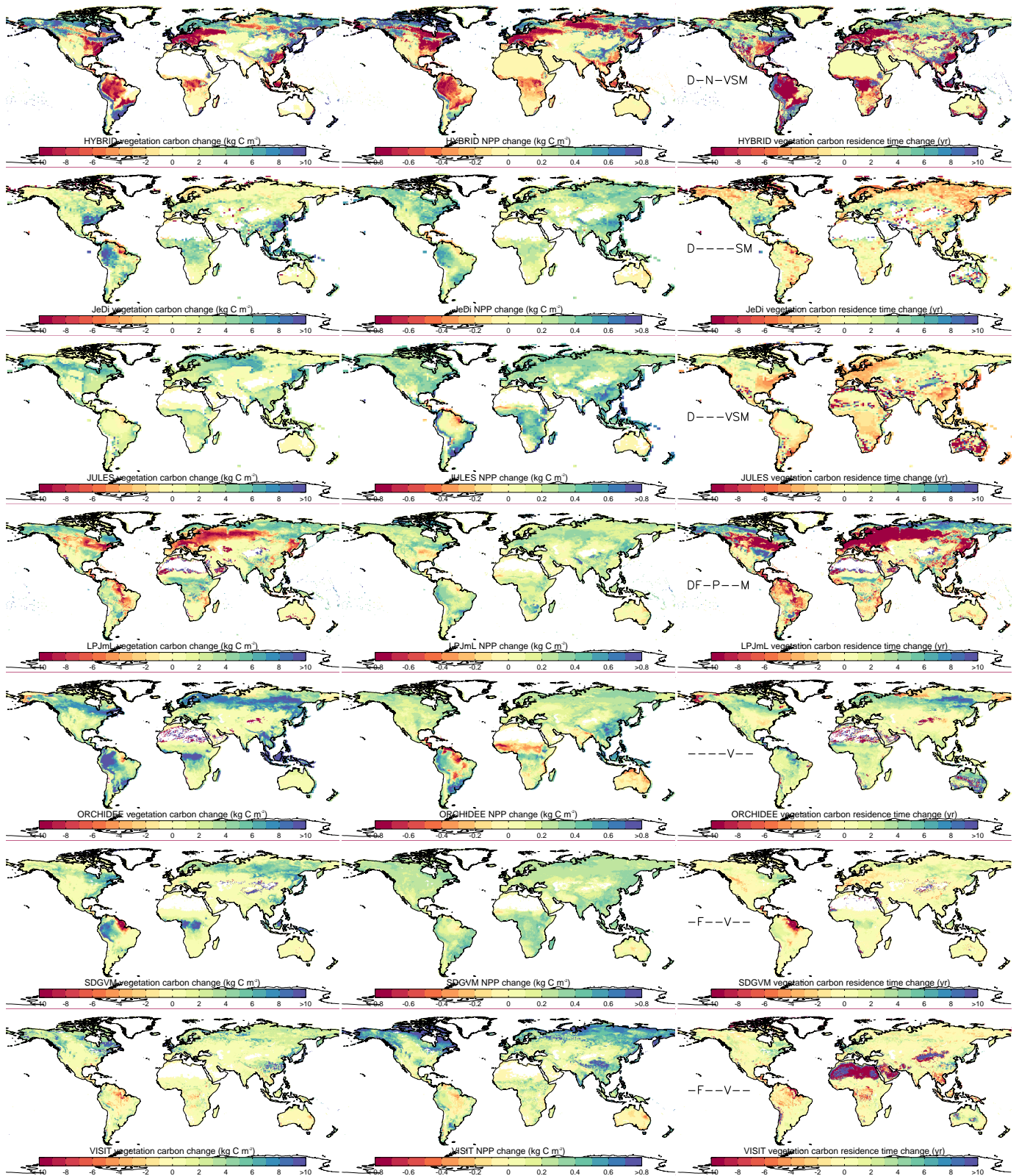
Fig. 4: Change in mean-decadal vegetation carbon, NPP, and vegetation carbon residence time simulated by seven GVMs under HadGEM2-ES RCP 8.5 forcings between A.D 2005 and 2099. Letters on right hand side panels indicate relevant processes for residence time and NPP behaviour included in each model: D = dynamic vegetation; F = fire; N = N cycle; P = permafrost; V = VPD affects stomatal conductance; S = temperature affects senescence; and M = temperature affects mortality.
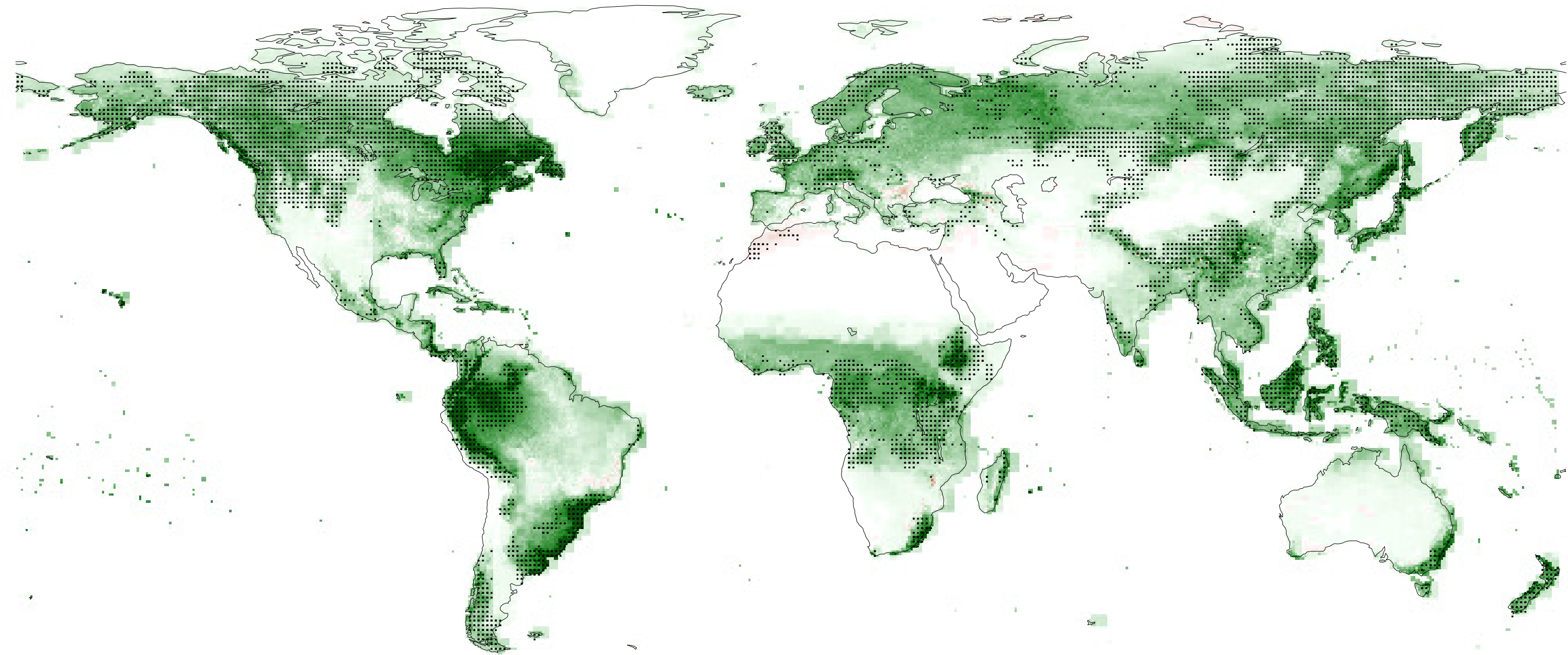
Vegetation carbon change between A.D. 1971–1999 and decades with +4 °C mean land warming (kg C m^{-2})

−5   5

A

|	HYBRID
	JeDi
	JULES
	LPJmL
	ORCHIDEE
	SDGVM
	VISIT

ΔVegetation Carbon (Pg C)
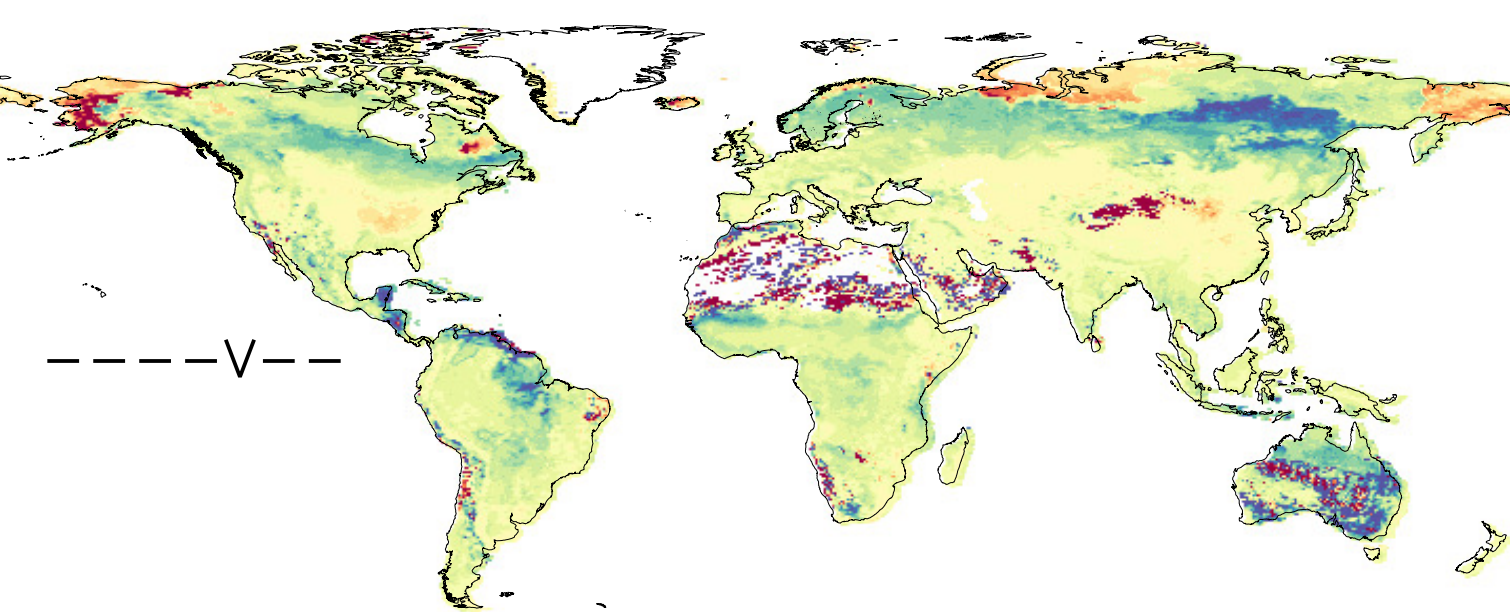
Year
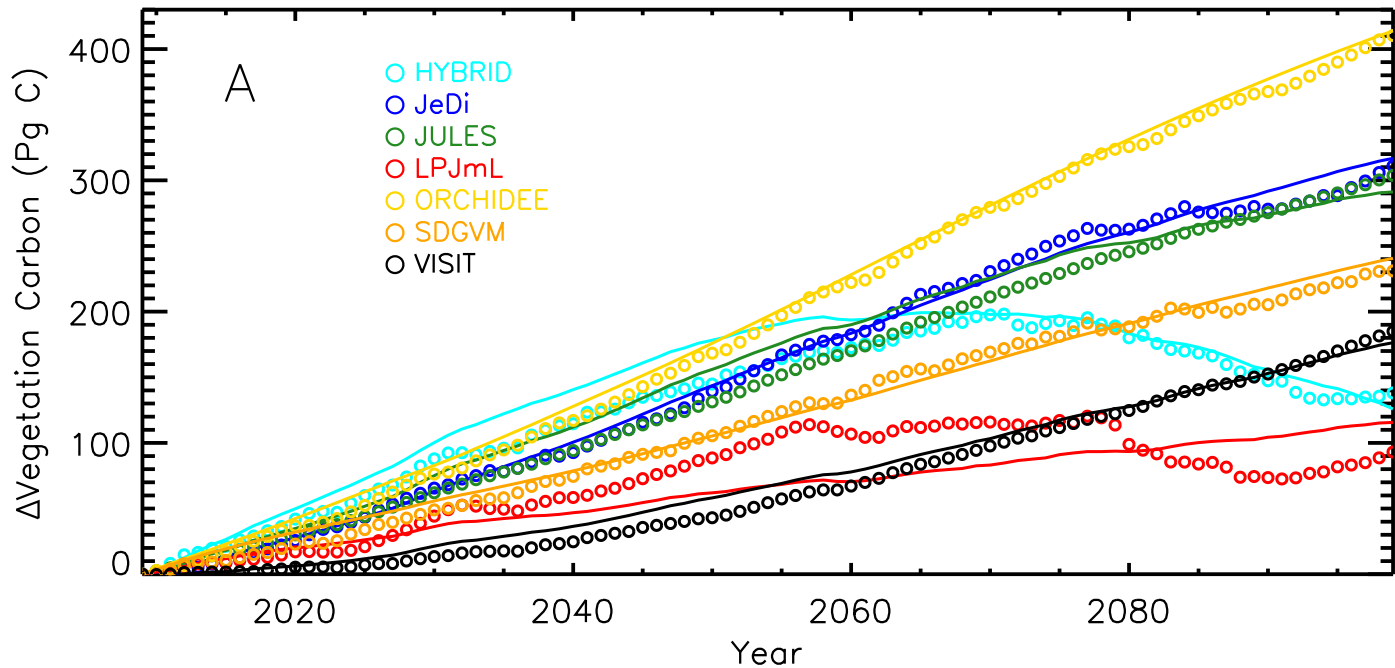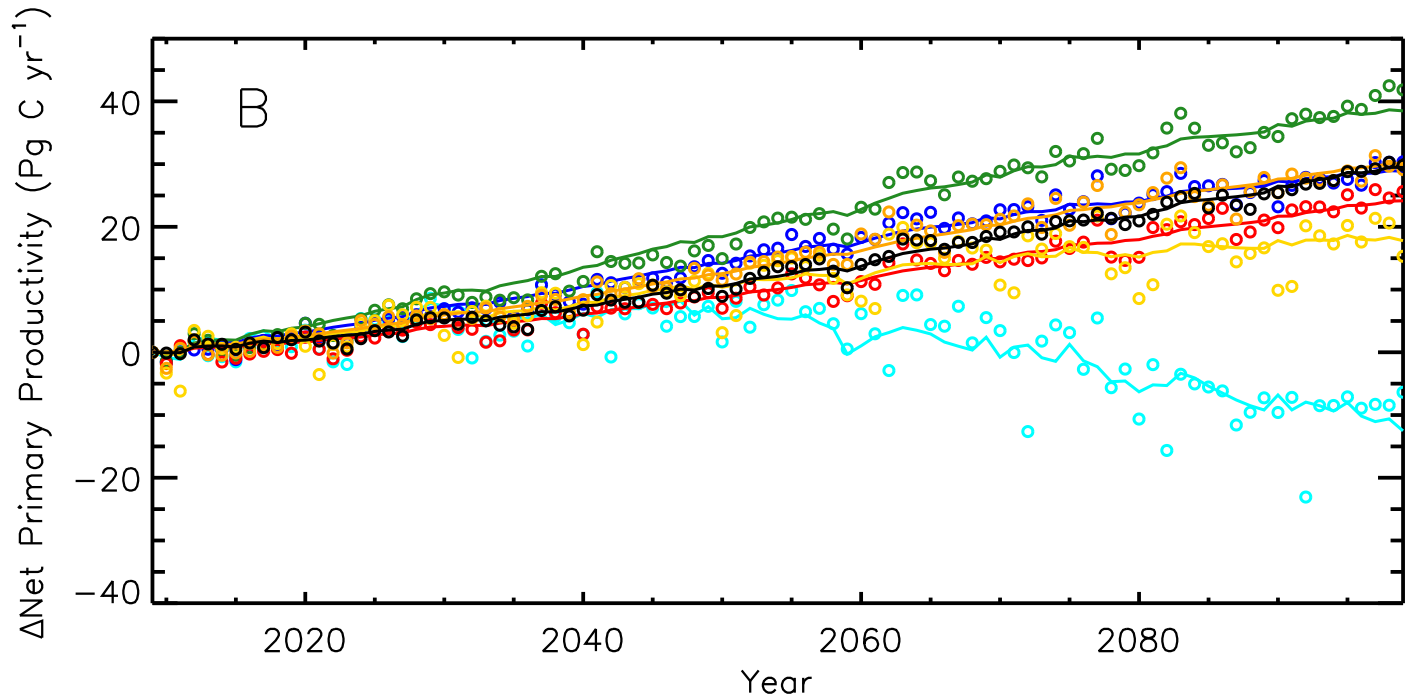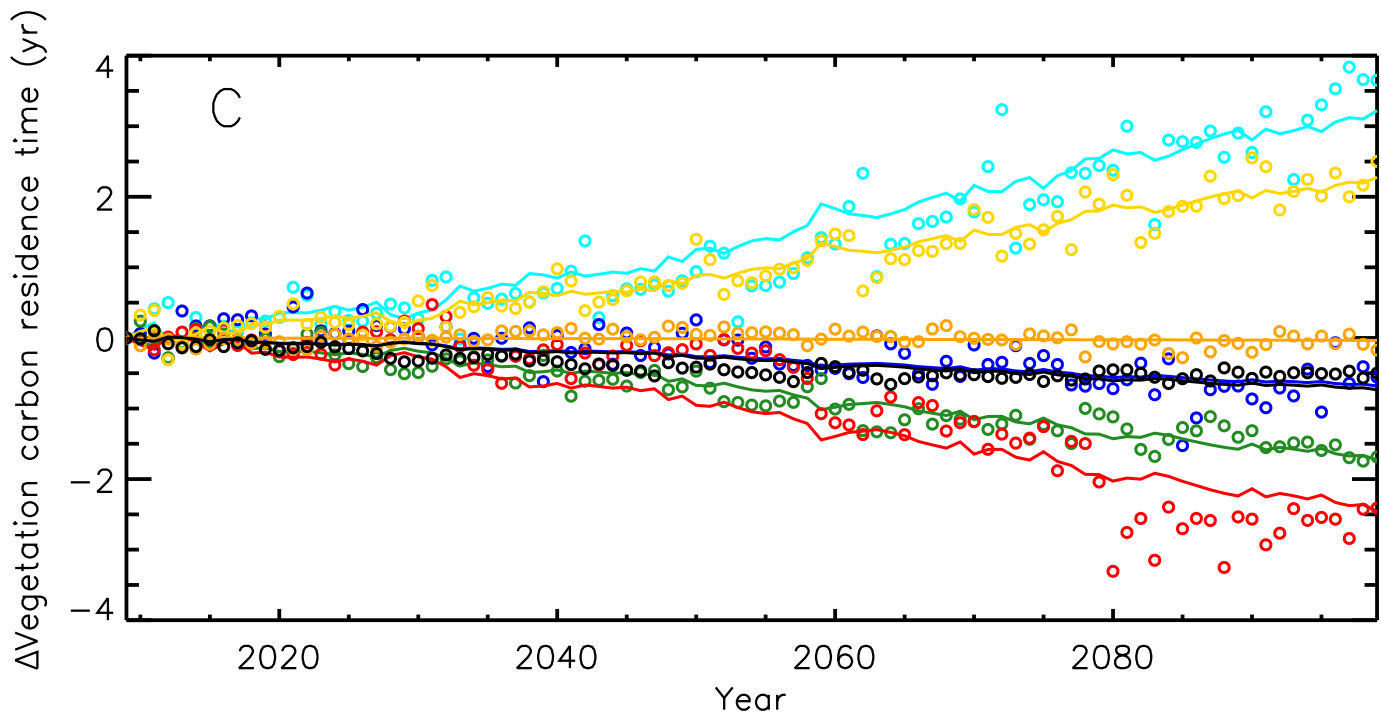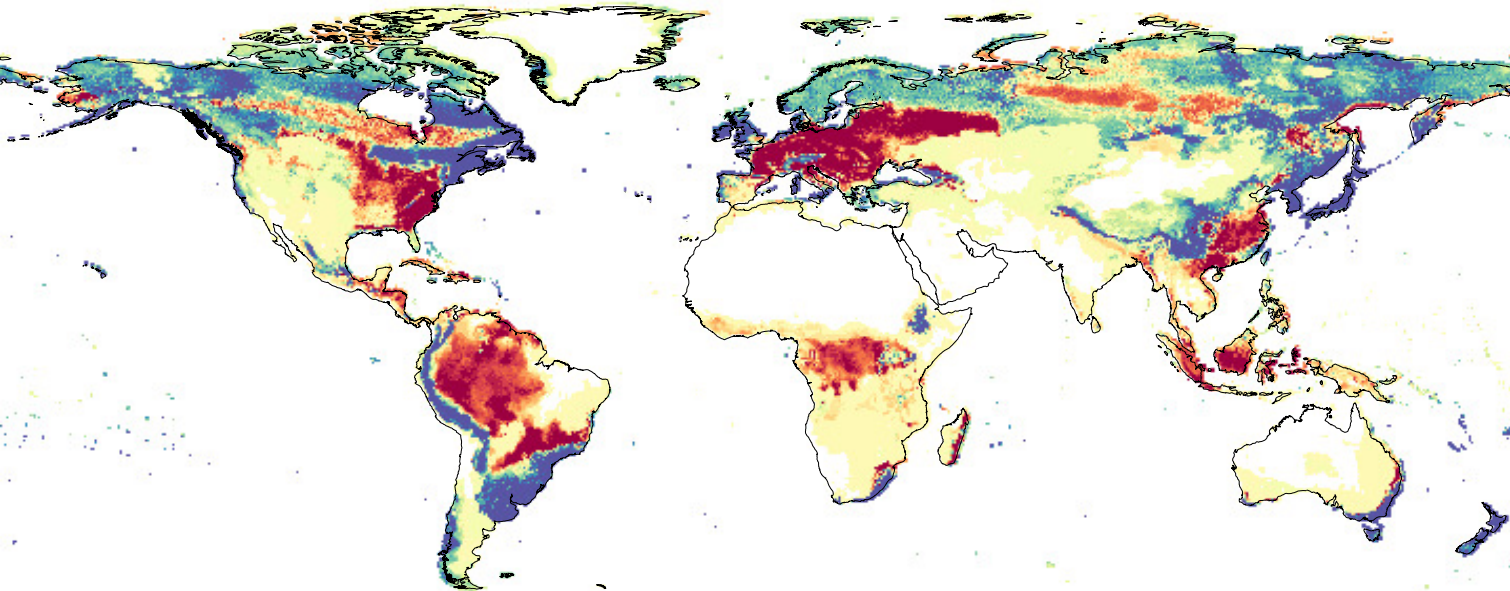
HYBRID vegetation carbon change (kg C m^{-2})
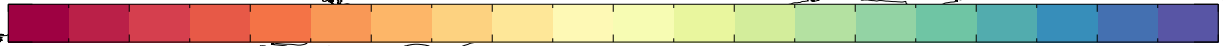
-10   -8   -6   -4   -2   0   2   4   6   8   >10
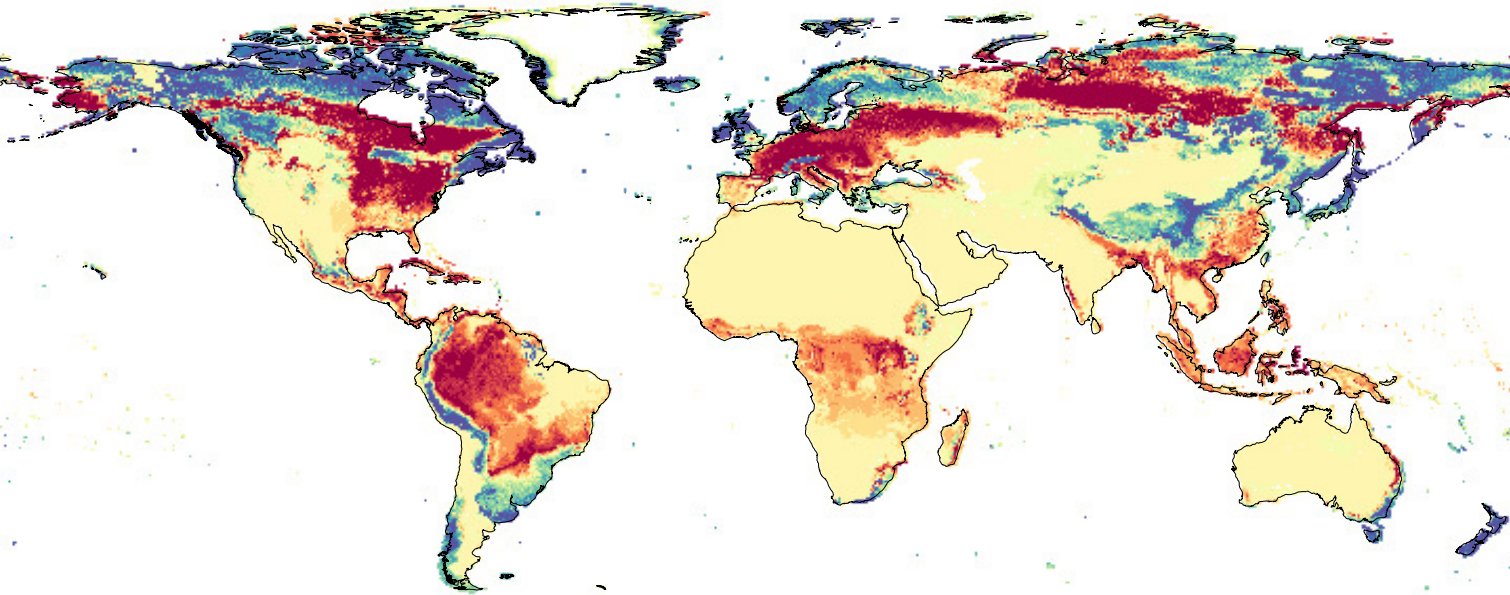
HYBRID NPP change (kg C m^{-2})
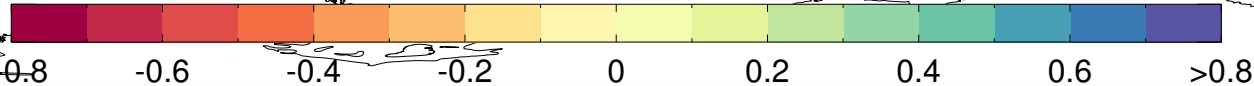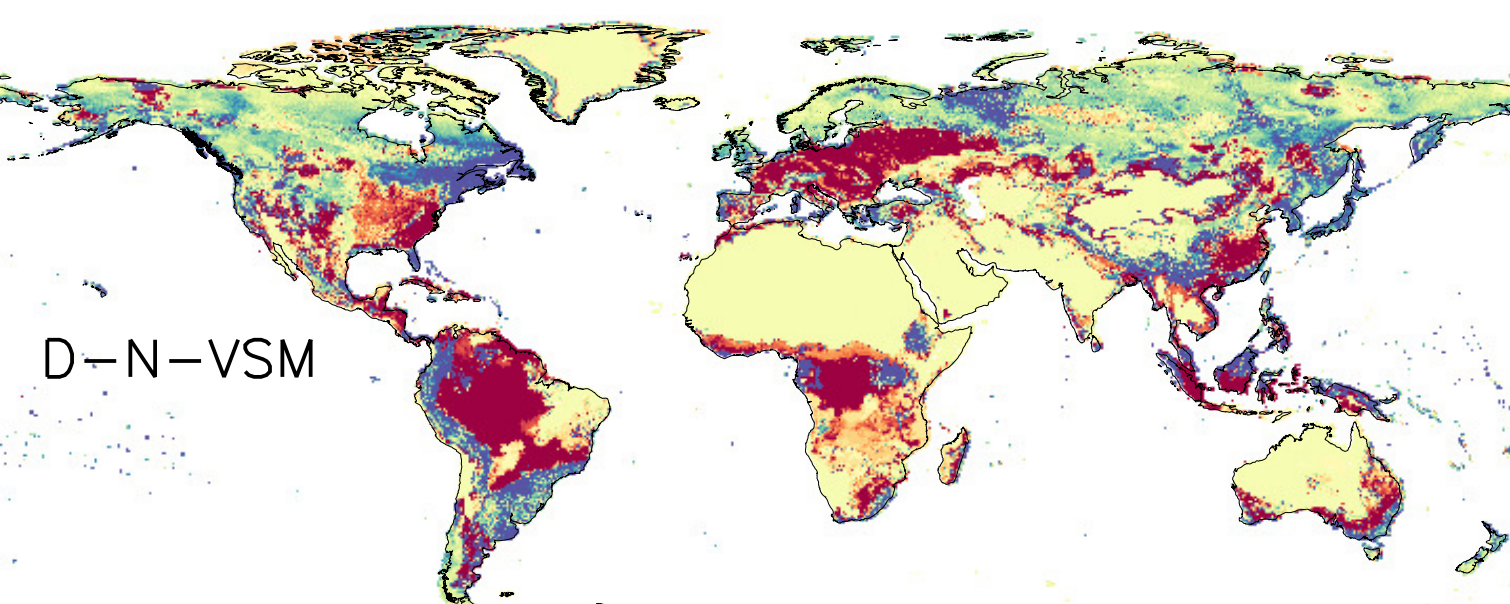
D−N−VSM

HYBRID vegetation carbon residence time change (yr)

<−10   -8   -6   -4   -2   0   2   4   6   8   >10

JeDi vegetation carbon change (kg C m^{-2})

-10   -8   -6   -4   -2   0   2   4   6   8   >10
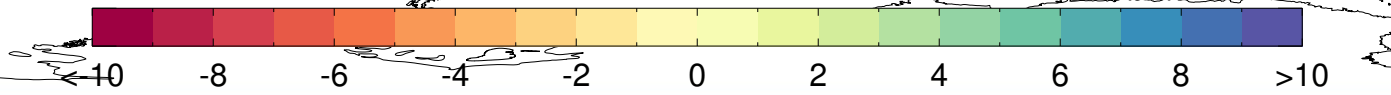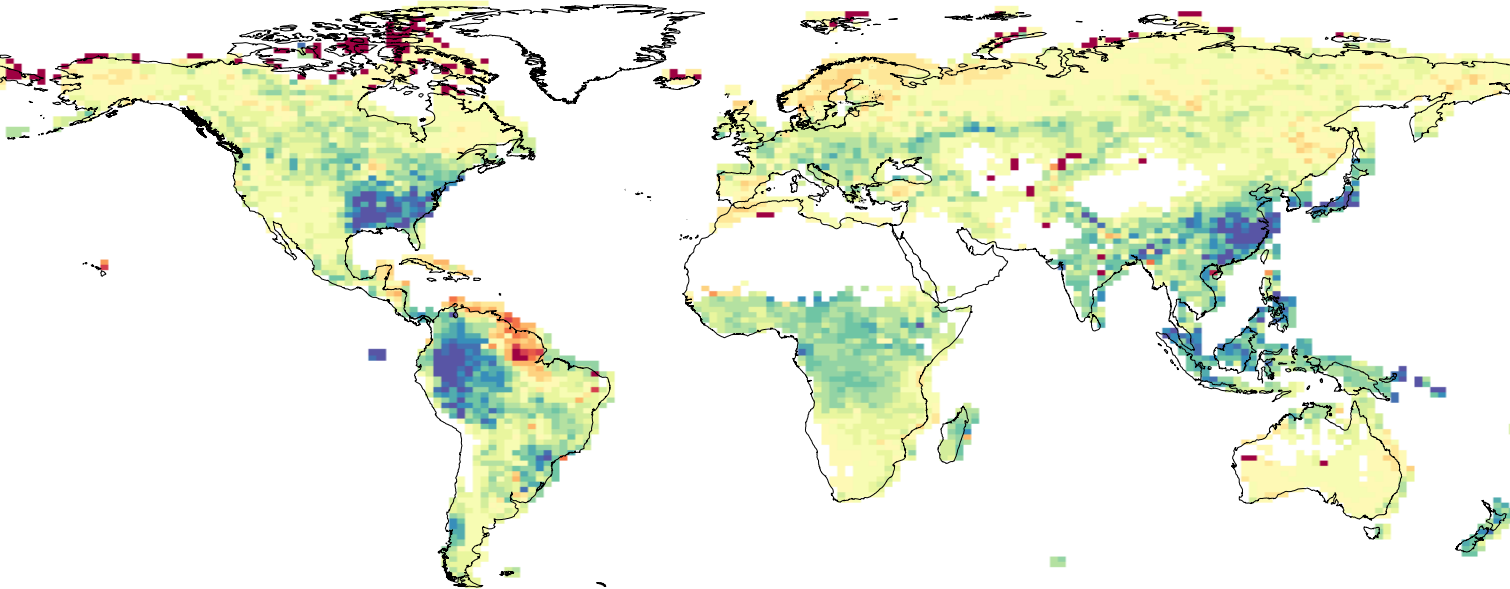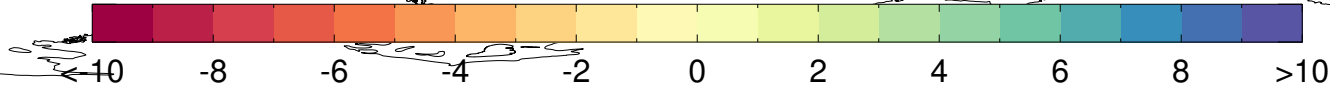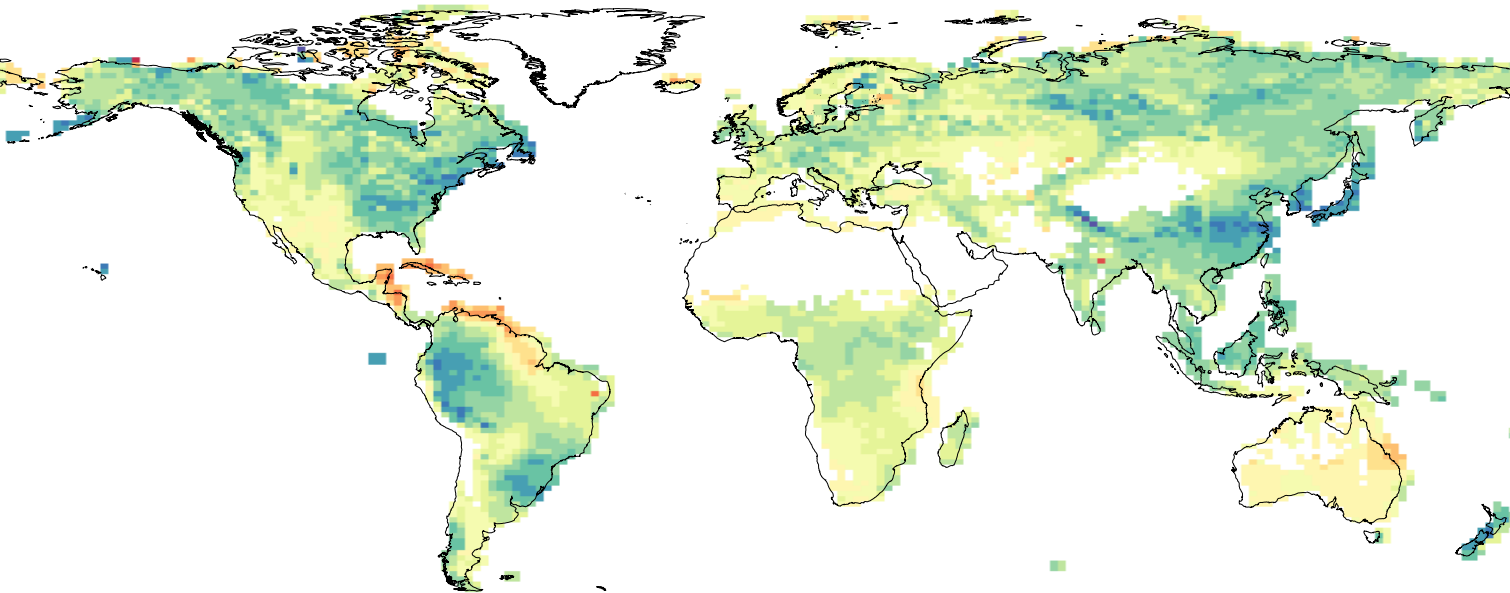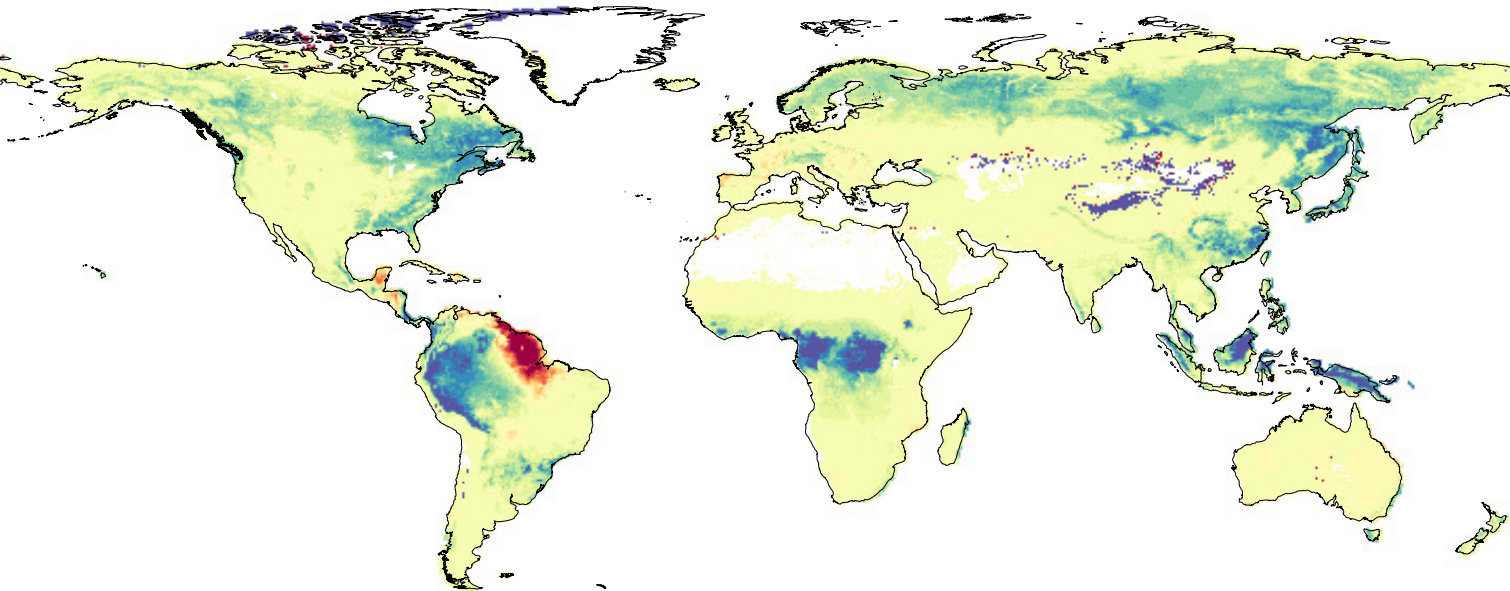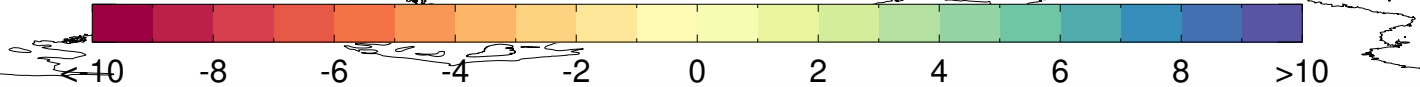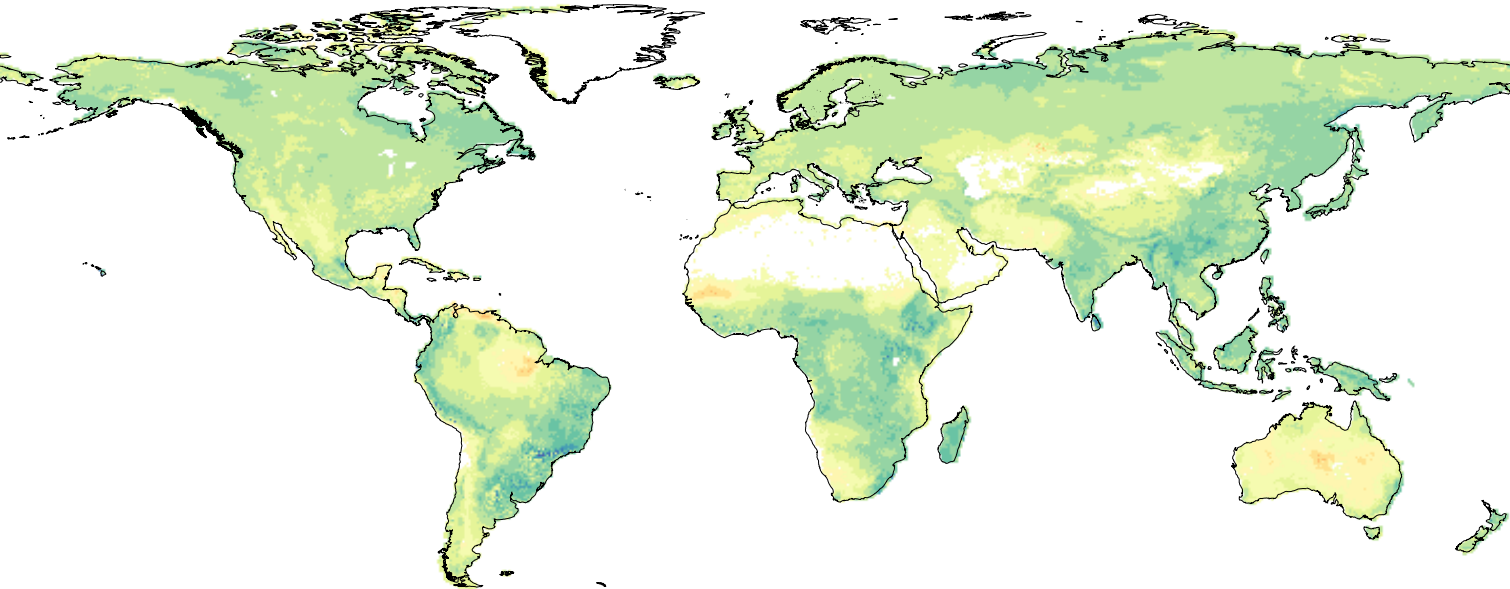
JeDi NPP change (kg C m^{-2})
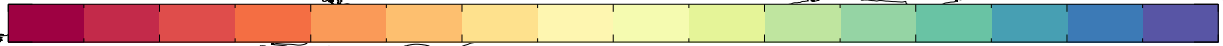
< -0.8   -0.6   -0.4   -0.2   0   0.2   0.4   0.6   > 0.8

JeDi vegetation carbon residence time change (yr)

D – – – – SM
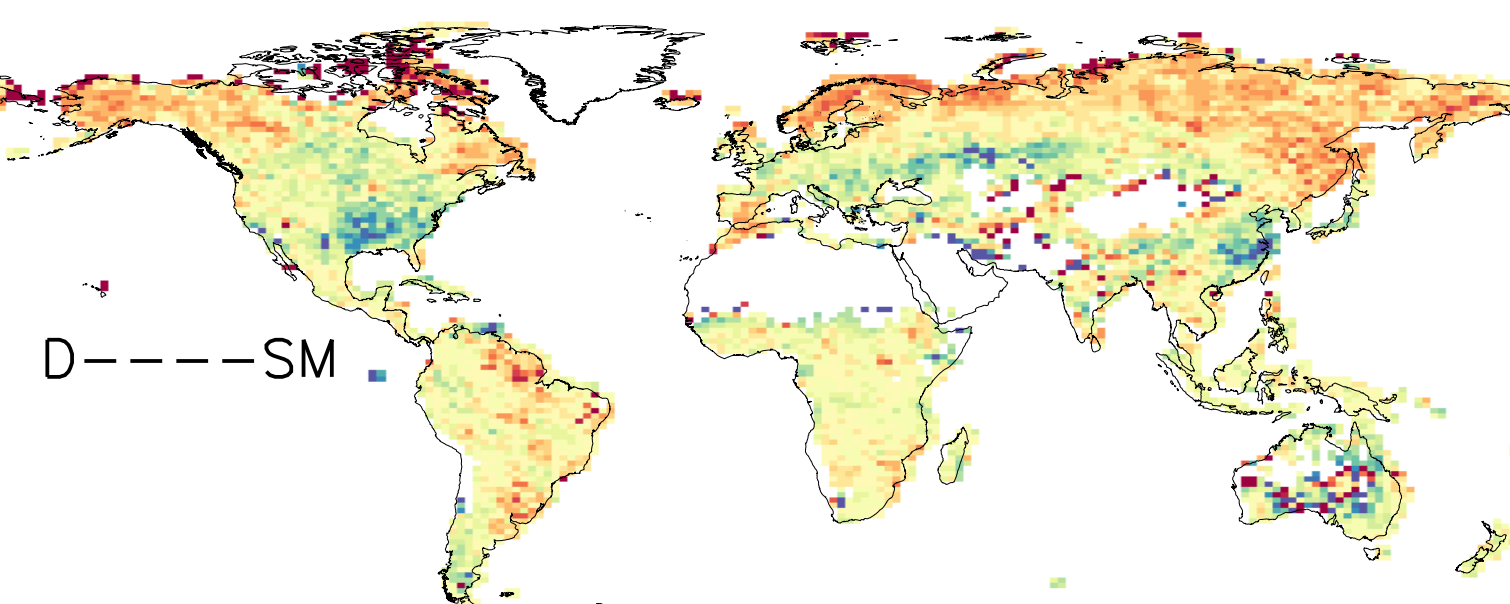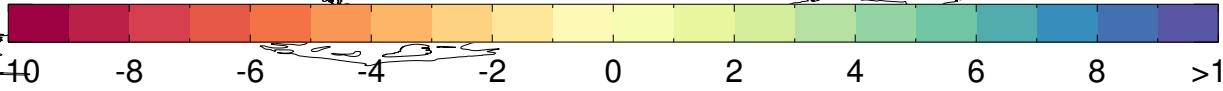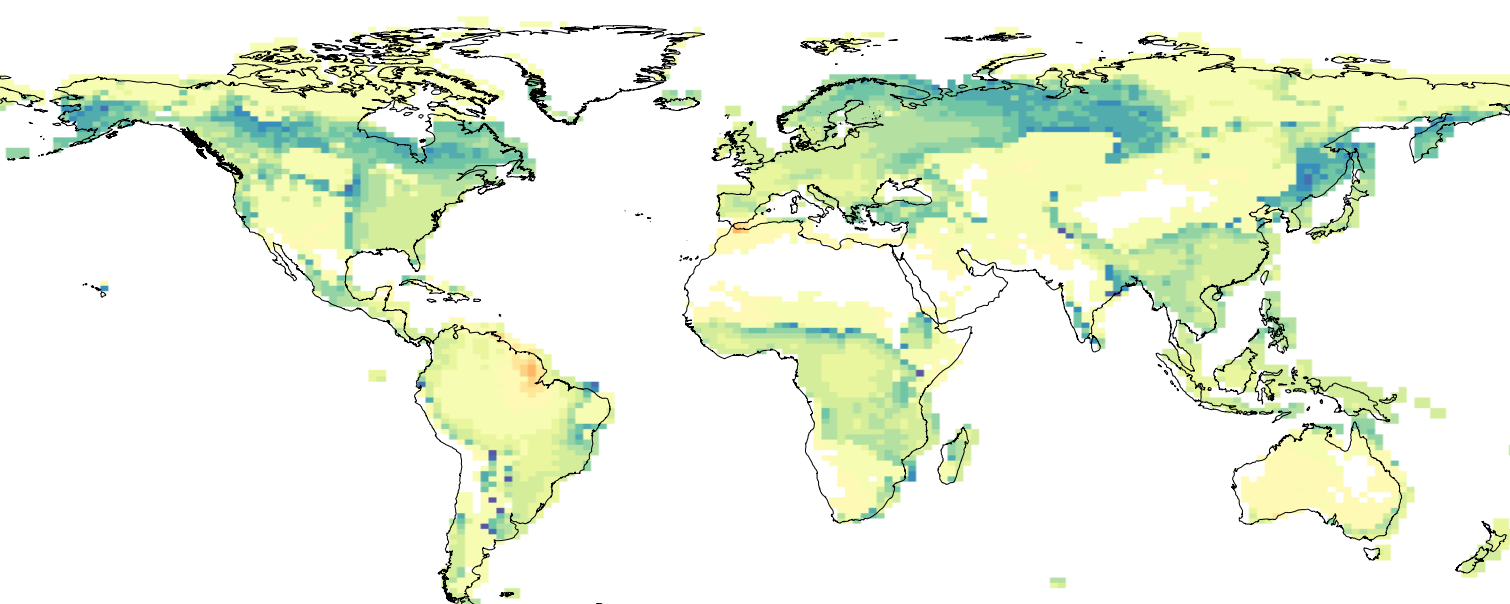
JULES vegetation carbon change (kg C m^{-2})
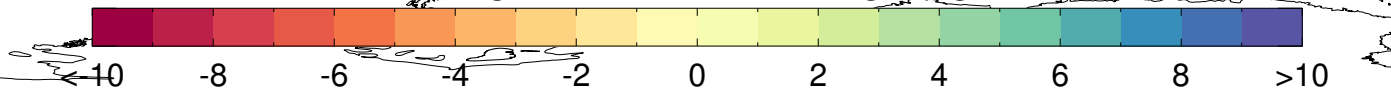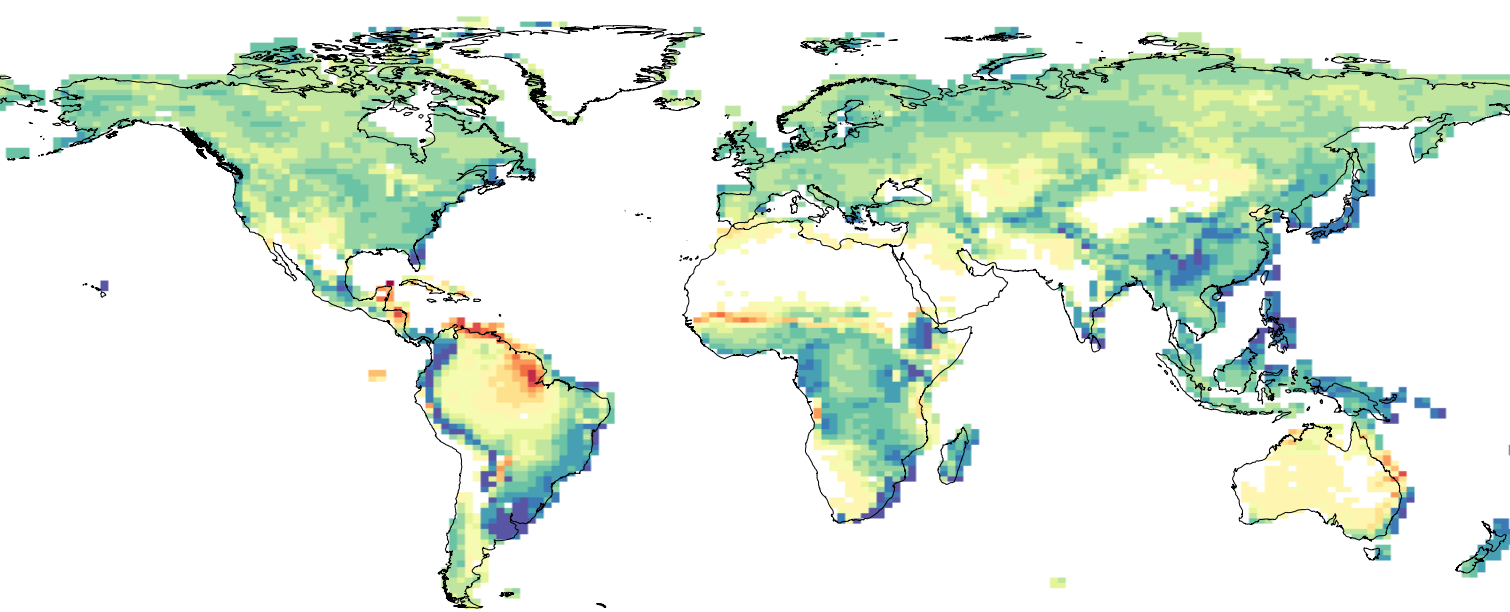
JULES NPP change (kg C m^{-2})
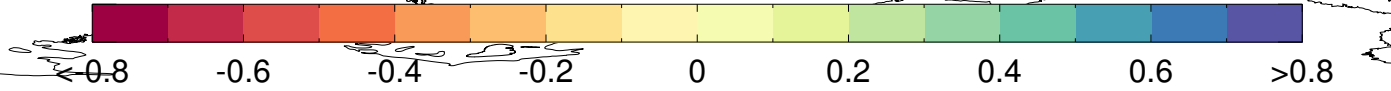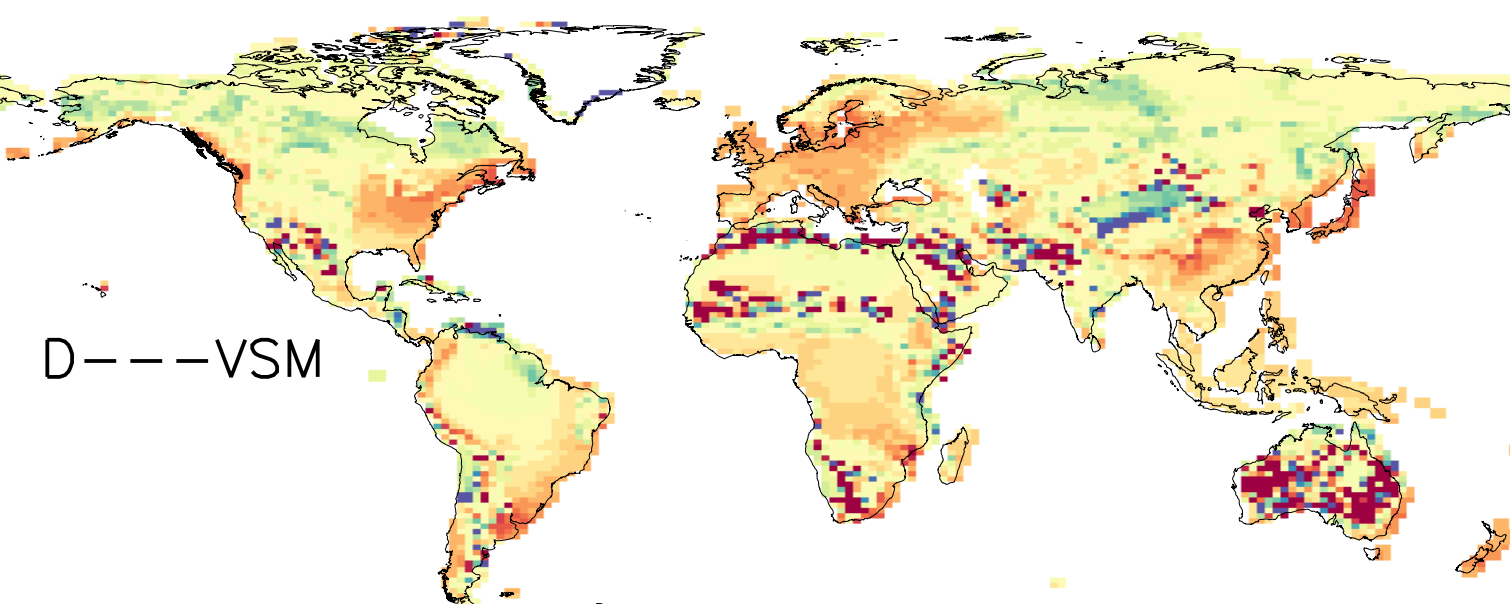
D - - - VSM

JULES vegetation carbon residence time change (yr)
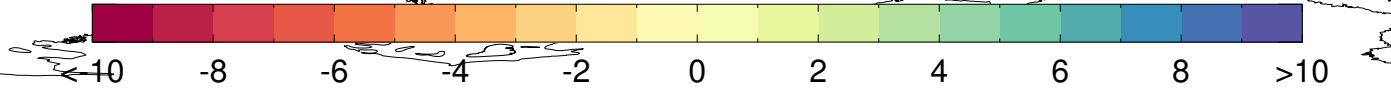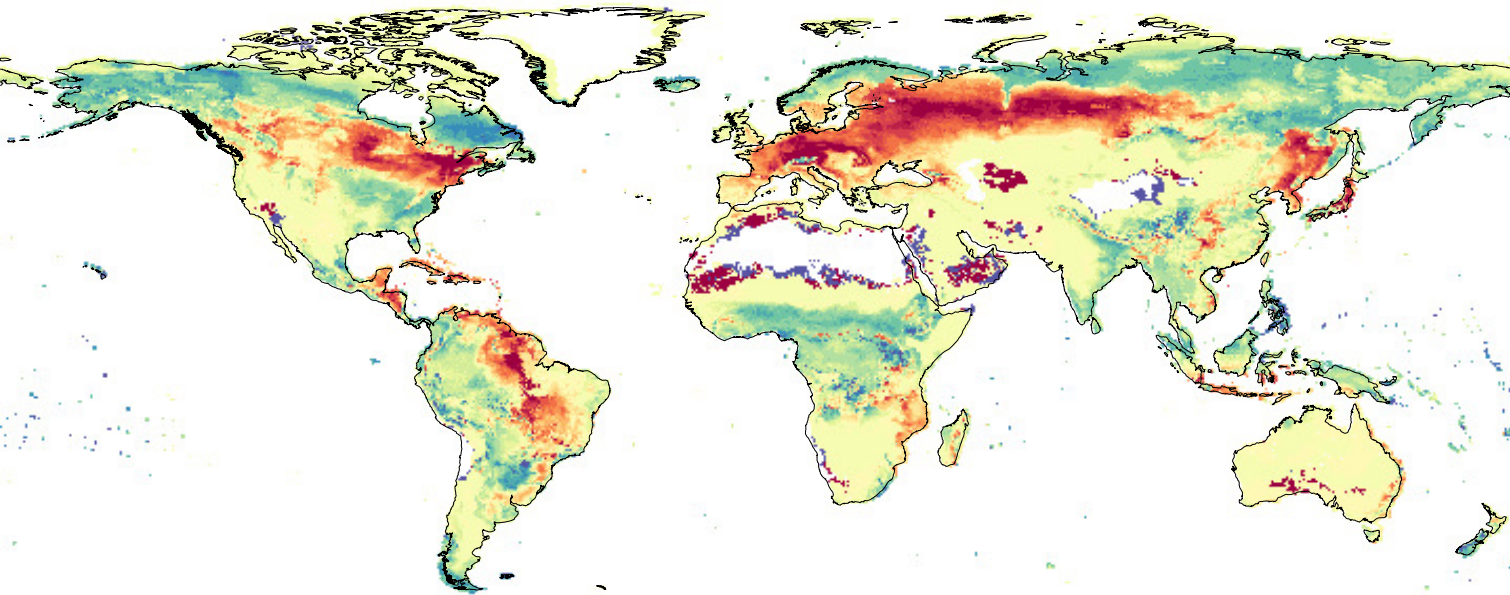
<-10 -8 -6 -4 -2 0 2 4 6 8 >10

LPJmL vegetation carbon change (kg C m^{-2})
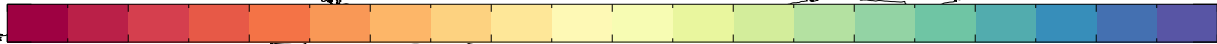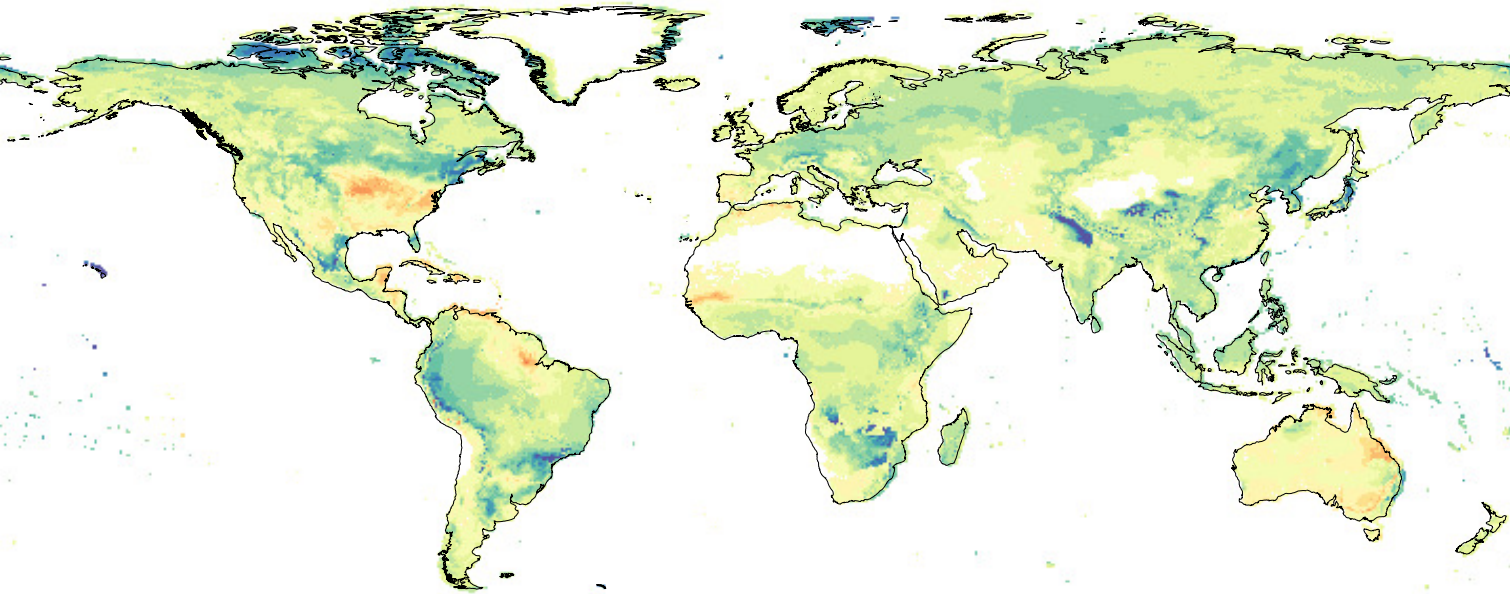
| <-10 | -8 | -6 | -4 | -2 | 0 | 2 | 4 | 6 | 8 | >10 |

LPJmL NPP change (kg C m^{-2})

<-0.8   -0.6   -0.4   -0.2   0   0.2   0.4   0.6   >0.8
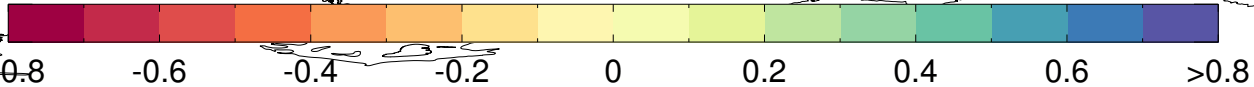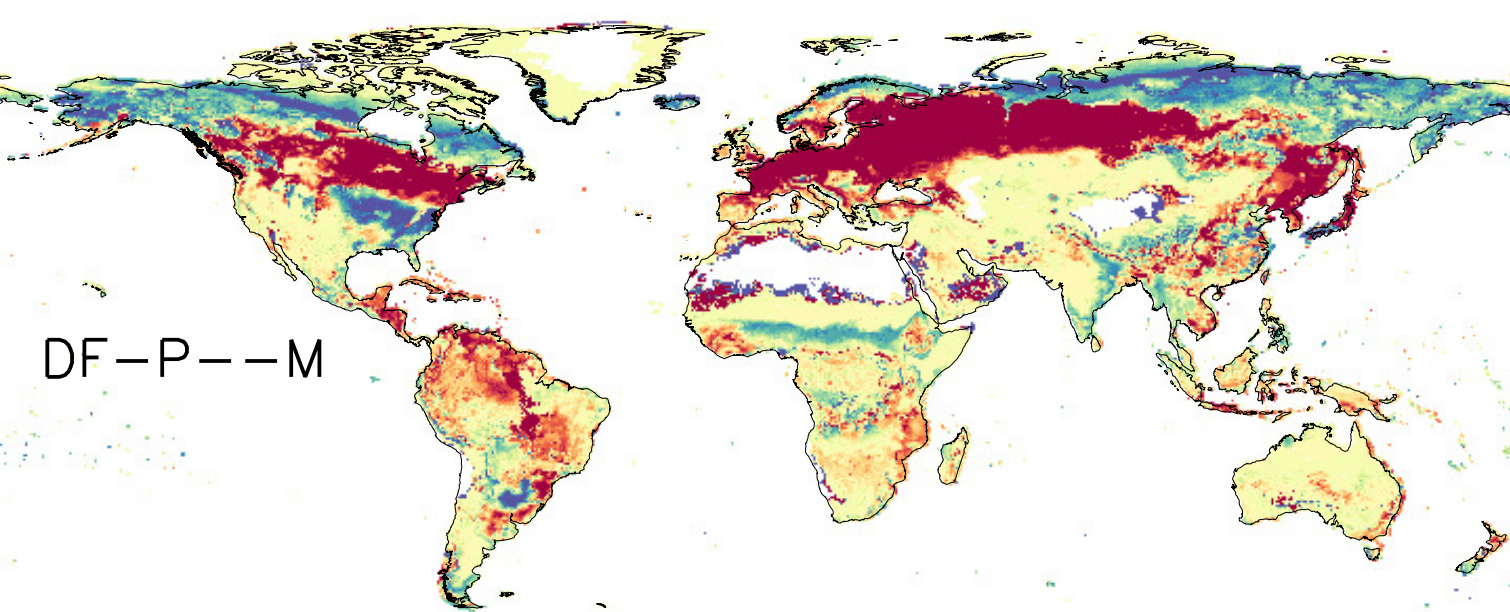
DF $-$ P $-$ $-$ M

LPJmL vegetation carbon residence time change (yr)
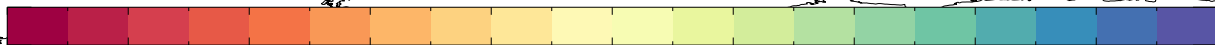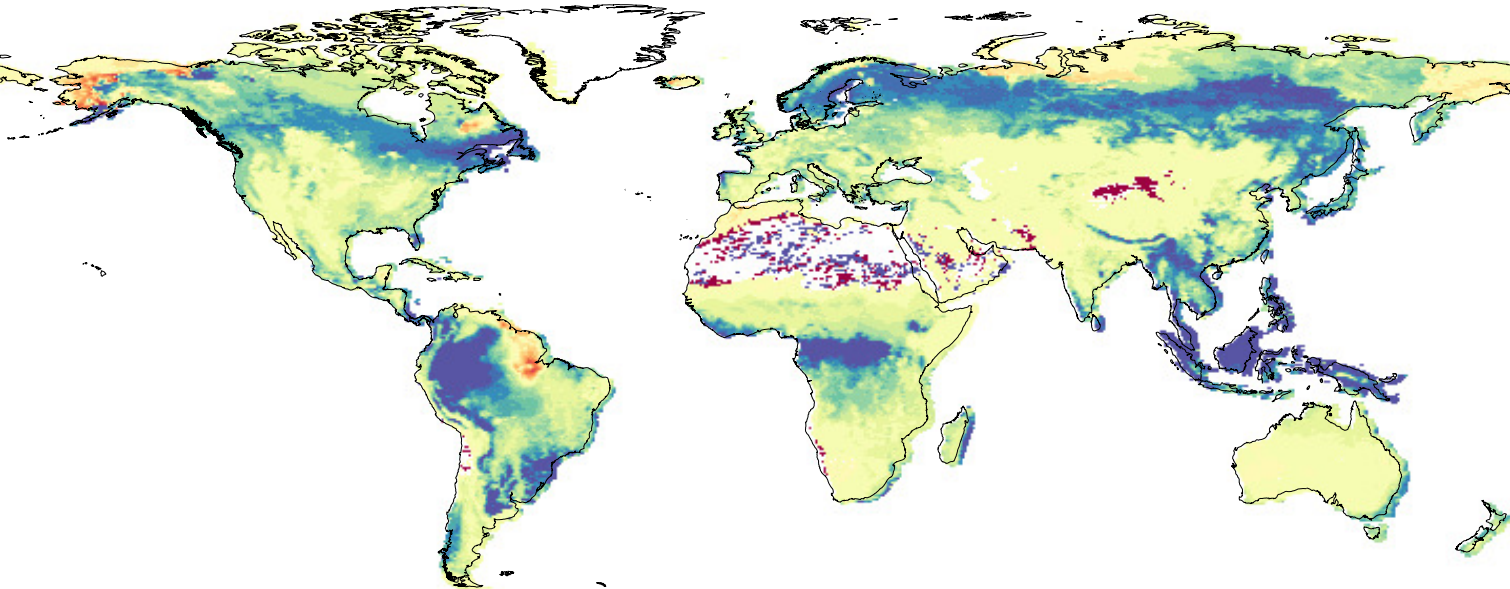
| <-10 | -8 | -6 | -4 | -2 | 0 | 2 | 4 | 6 | 8 | >10 |

ORCHIDEE vegetation carbon change (kg C m^{-2})
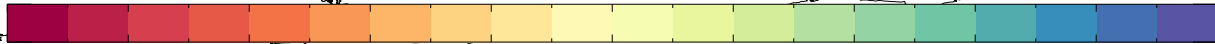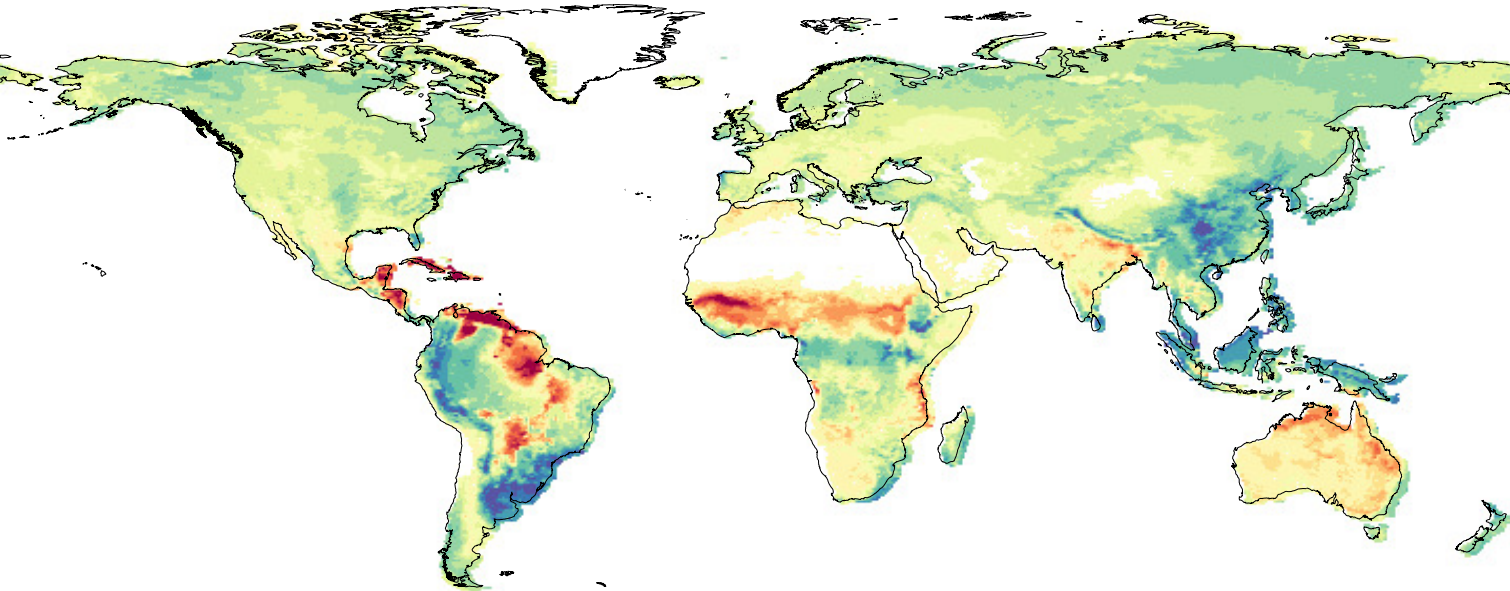
-10   -8   -6   -4   -2   0   2   4   6   8   >10

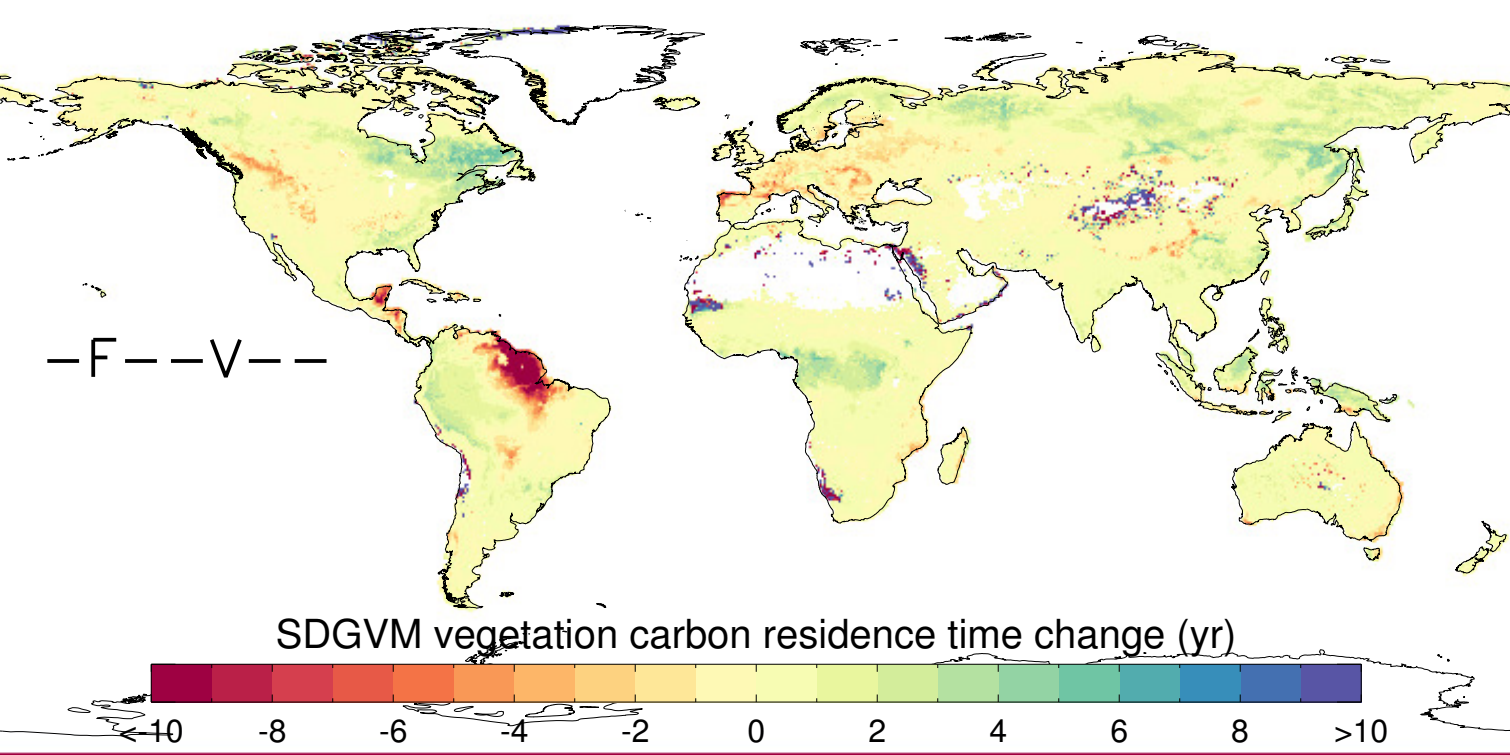ORCHIDEE NPP change (kg C m^{-2})
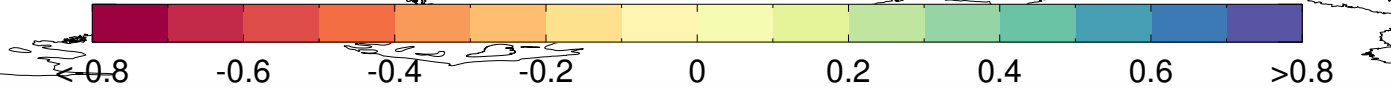
ORCHIDEE vegetation carbon residence time change (yr)
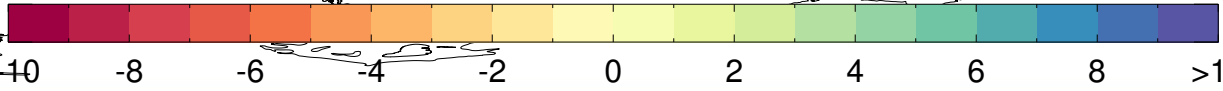
< -10   -8   -6   -4   -2   0   2   4   6   8   >10

SDGVM vegetation carbon change (kg C m^{-2})
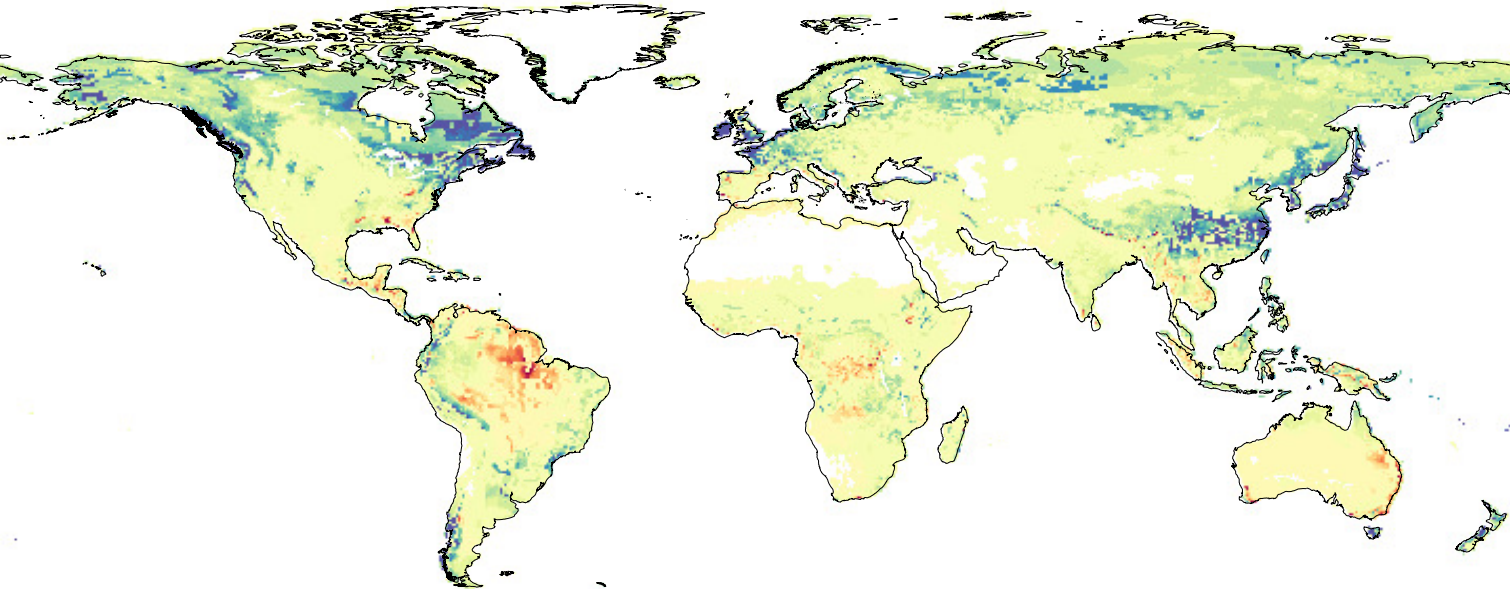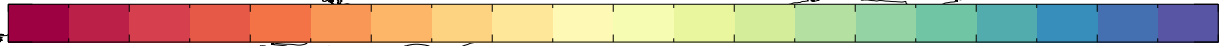
| <-10 | -8 | -6 | -4 | -2 | 0 | 2 | 4 | 6 | 8 | >10 |

SDGVM NPP change (kg C m^{-2})

SDGVM vegetation carbon residence time change (yr)
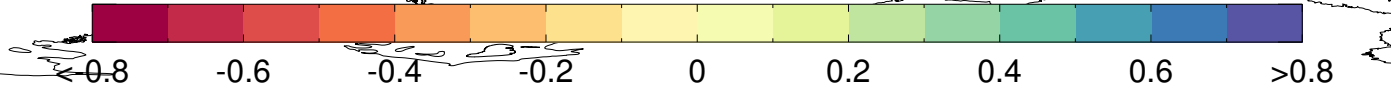
| <-10 | -8 | -6 | -4 | -2 | 0 | 2 | 4 | 6 | 8 | >10 |

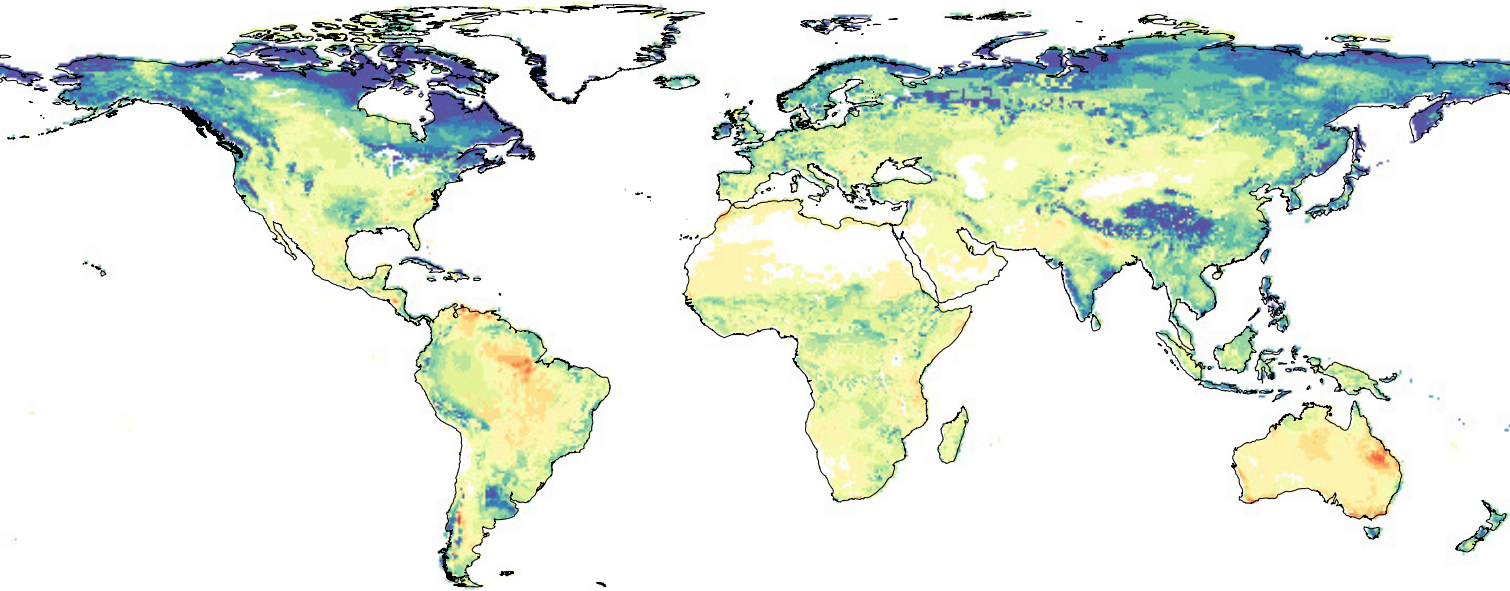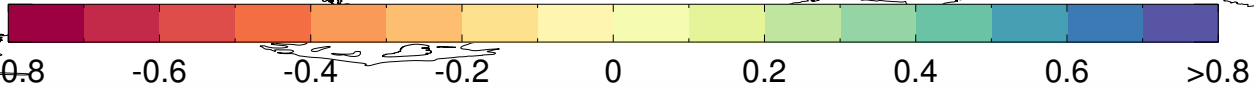VISIT vegetation carbon change (kg C m^{-2})

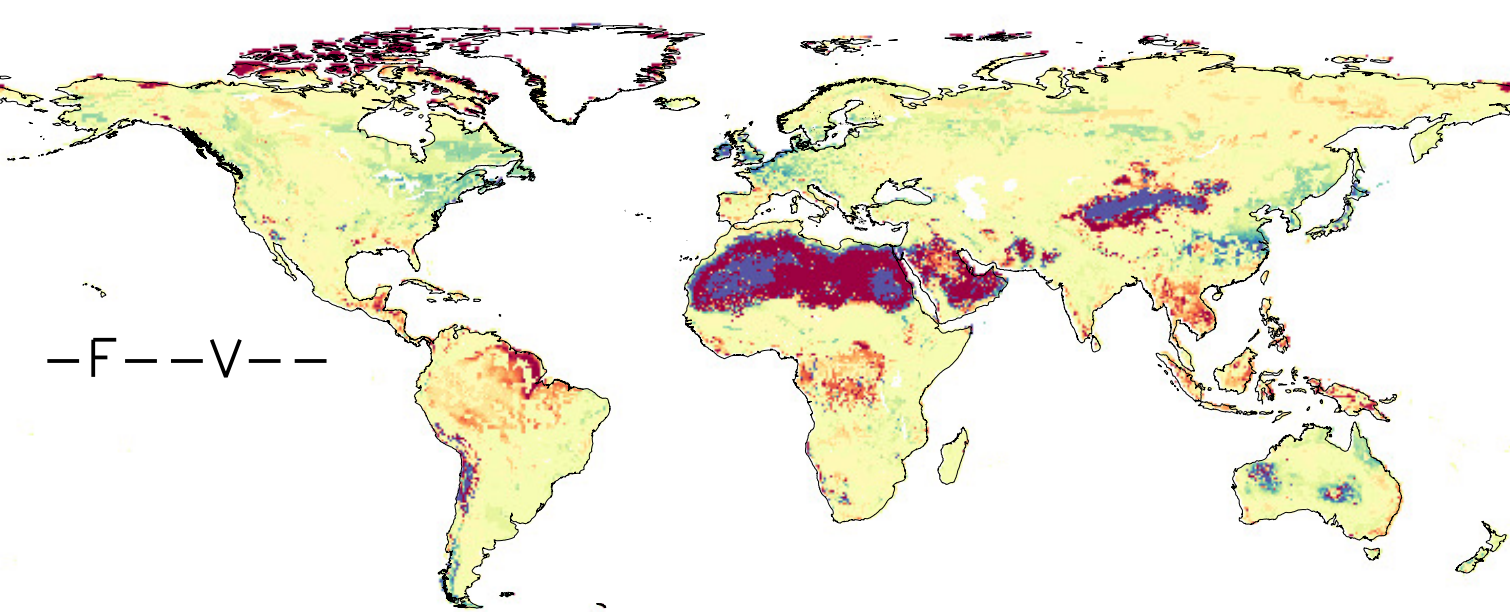-10   -8   -6   -4   -2   0   2   4   6   8   >10

VISIT NPP change (kg C m^{-2})

| <-0.8 | -0.6 | -0.4 | -0.2 | 0 | 0.2 | 0.4 | 0.6 | >0.8 |

VISIT vegetation carbon residence time change (yr)

‹−10   −8   −6   −4   −2   0   2   4   6   8   >10